BIOSYSTEMS ENGINEERING XXX (2009) 1–19

Available at www.sciencedirect.com

journal homepage: www.elsevier.com/locate/issn/15375110

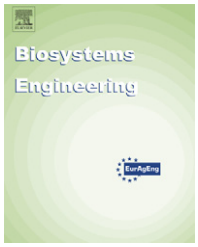

Research Paper: SE—Structures and Environment

A study of natural ventilation in an Almería-type greenhouse with insect screens by means of tri-sonic anemometry

F.D. Molina-Aiz[a,*], D.L. Valera[a], A.A. Peña[a], J.A. Gil[b], A. López[a]

[a]Departamento de Ingeniería Rural, Universidad de Almería, Escuela Politécnica Superior, Ctra. Sacramento, 04120 Almería, Spain
[b]Departamento de Ingeniería Rural, E.T.S.I. Agrónomos y de Montes, Universidad de Córdoba, Campus de Rabanales, Nacional IV km 396, 14071 Córdoba, Spain

ARTICLE INFO

Article history:
Received 23 May 2007
Received in revised form
31 May 2009
Accepted 9 June 2009
Published online ■

The wind coefficient of an Almería-type greenhouse has been calculated from direct estimation of airflow at the openings by means of three-dimensional sonic anemometry. Measurements were taken with a strong northeast wind (*Levante*) and with a weak westerly wind (*Poniente*). For the model considering only the wind effect, the coefficient of effectiveness obtained was $E_V = C_d C_w^{0.5} = 0.050$, and the values of the mean and turbulent wind coefficients were $C_w = 0.066$ and $C_w' = 0.029$, respectively. Two important characteristics of the Almería-type greenhouse analysed in this work make natural ventilation difficult: the presence of mature tomato plants inside the greenhouse and of an obstacle close to one of the side openings, which affected the air movement throughout it. Discharge coefficients due to the presence of screens in the greenhouse ($C_{d,\varphi} = 0.156$–0.245) were calculated from wind-tunnel measurements, obtaining a total discharge coefficient of $C_d = 0.193$. Use of the anti-aphid screen in the openings can cause an approximately 71% reduction of C_d and consequently of the wind-related coefficient E_V. Winds perpendicular to the axis produce an inflow through the side opening free of obstacles and an outflow through the roof vents. In qualitative terms, this airflow pattern is in good agreement with previous simulations using Computational Fluid Dynamics.

1. Introduction

Natural ventilation is the main means of climate control in the greenhouses which cover over 27 000 hectares in the Spanish province of Almería. However, there is still very little information available on the design of Almería-type greenhouses with natural ventilation. In recent years, the Almería-type greenhouse has been exported to other countries and warm climate areas such as Mexico, Colombia, Morocco and China. In hot summer conditions, deficient ventilation makes control of the air temperature in the plant zone difficult. The air velocity usually observed in the plant zone inside naturally ventilated greenhouses is around 0.1–0.5 m s^{-1} (Bartzanas *et al.*, 2004; Molina-Aiz *et al.*, 2004a,b; Jiménez-Hornero *et al.*, 2005; Soni *et al.*, 2005; Teitel *et al.*, 2005; Fatnassi *et al.*, 2006).

Given the importance of natural ventilation in greenhouse climate control, many research works have attempted to establish a numerical function which directly relates ventilation rates to different environmental variables, such as wind speed and direction, solar radiation or interior and exterior temperature. To date, most studies on natural ventilation have been based on estimations of a total exchange rate of air

* *Corresponding author.* .
E-mail addresses: fmolina@ual.es (F.D. Molina-Aiz), gilribes@uco.es (J.A. Gil).
1537-5110/$ – see front matter © 2009 IAgrE. Published by Elsevier Ltd. All rights reserved.
doi:10.1016/j.biosystemseng.2009.06.013

Nomenclature

a, b, c	second-order polynomial regression coefficients
A, B, C	parameters used to calculate the ratio of the mean to the instantaneous ventilation flux
C_d	total discharge coefficient of the opening
$C_{d,LH}$	discharge coefficient due to the shape of the opening
$C_{d,\varphi}$	discharge coefficient due to the presence of insect-proof screens
C_w	wind effect coefficient for the mean airflow
C_w'	wind effect coefficient for the turbulence airflow
D	pore height, mm
d	wire diameter of the insect-proof screen, mm
E_V	coefficient of effectiveness of the openings
e	thickness of the screen, m
F_φ	pressure drop coefficient due to the presence of an insect-proof screen
$\overline{G}$	mean volumetric flow rate, $m^3 s^{-1}$
G'	turbulent component of the ventilation flow, $m^3 s^{-1}$
G_T	free component of the ventilation flux induced by buoyancy forces, $m^3 s^{-1}$
G_w	forced component of the ventilation flux induced by wind forces, $m^3 s^{-1}$
g	gravitational acceleration, $m s^{-2}$
H	vent opening height, m
HR	relative air humidity, %
h_{SR}	difference in height between side and roof openings, m
i_y, i_z	turbulence intensity in directions y and z
K_p	screen permeability, m^2
L	length of the window, m
P	pressure, Pa
R	ventilation rate, h^{-1}
Re_p	Reynolds number based on the screen's permeability
R_g	global radiation outside the greenhouse, $W m^{-2}$
S_c	greenhouse area, m^2
S_V	surface area of the vent openings, m^2
T	air temperature, °C
$\overline{T}$	mean air temperature, °C
u	air velocity, $m s^{-1}$
$\overline{u}$	mean air velocity, $m s^{-1}$
u'	fluctuating air velocity, $m s^{-1}$
$\ddot{u}$	air velocities scaled only with wind speed, $m s^{-1}$
u^*	air velocities scaled with wind speed and temperature differences, $m s^{-1}$
U_o	wind speed at reference height (4 m), $m s^{-1}$
W	pore width, mm
Y	inertial factor
α	angle of opening, degree
ΔG	difference between the volumetric flow rate entering and exiting through the openings, $m^3 s^{-1}$
ΔT_{io}	inside to outside temperature difference, °C
μ	dynamic viscosity of air, $kg s^{-1} m^{-1}$
θ	wind direction, degree
φ	insect-proof screen porosity
ρ	air density, $kg m^{-3}$
σ_u	standard deviation of the air velocity, $m s^{-1}$

Subscripts

i	inside
L	leeward
M	average value
o	outside
R	roof vent
S	side vent
W	windward

using gas tracer techniques (Bot, 1983; Fernandez and Bailey, 1992; Boulard and Draoui, 1995; Kittas *et al.*, 1995; Papadakis *et al.*, 1996; Kittas *et al.*, 1996; Baptista *et al.*, 1999; Kittas *et al.*, 2002) and simulations of homogeneous air temperature by means of energy balance models (Wang and Boulard, 2000; Demrati *et al.*, 2001). Nevertheless, these techniques only allow prediction of a general air change rate in the greenhouse. Airflow has also been estimated directly through the vents by measuring the difference in pressure in different greenhouses (Kittas *et al.*, 1996; Boulard *et al.*, 1998). More recently, airspeed measurements have been taken through vents and inside the greenhouse using unidimensional (Boulard *et al.*, 1997b), two-dimensional (Wang and Deltour, 1999) or three-dimensional (3D) sonic anemometers (Wang and Deltour, 1997; Boulard *et al.*, 1998; Boulard *et al.*, 2000; Tanny *et al.*, 2006; Katsoulas *et al.*, 2007; Teitel *et al.*, 2008; Kittas *et al.*, 2008) and hot wire anemometry (Molina-Aiz *et al.*, 2004a,b). Some of these studies (Boulard *et al.*, 1996, 1997b) have shown the feasibility of direct measurements of airflow through the greenhouse vents. Teitel *et al.* (2008) calculated the ventilation rate by multiplying the average air velocity near the inlet and outlet openings (measured by a 3D sonic anemometer in the middle of the opening) by the area of the windows, obtaining ventilation rates similar to those obtained by N_2O tracer gas analysis.

Several authors have studied the reduction of ventilation airflow caused when the screens are installed on greenhouse openings (Sase and Christianson, 1990; Montero *et al.*, 1997; Teitel and Shklyar, 1998; Muñoz *et al.*, 1999; Fatnassi *et al.*, 2002; Bailey *et al.*, 2003; Pérez Parra *et al.*, 2004; Katsoulas *et al.*, 2006). Quantification of the screens' effect on ventilation has been studied using Bernoulli's approach, characterising their performance by a discharge coefficient (Kosmos *et al.*, 1993; Muñoz *et al.*, 1999; Teitel *et al.*, 1999; Fatnassi *et al.*, 2003) or using Forchheimer's equation (Miguel *et al.*, 1997; Valera *et al.*, 2006), considering screens as porous media characterised by permeability and inertial factor. The resistance of insect screens to airflow through greenhouse vent openings has also been analysed recently by experiments (Teitel, 2001; Kittas *et al.*, 2002; Tanny *et al.*, 2003; Soni *et al.*, 2005; Harmanto *et al.*, 2006; Kittas *et al.*, 2006) and numerical models of Computational Fluid Dynamics (CFD) (Bartzanas *et al.*, 2002; Fatnassi *et al.*, 2003; Molina-Aiz *et al.*, 2005; Fatnassi *et al.*, 2006).

With a view to characterising natural ventilation in a five-span Almería-type greenhouse, the mean and turbulent

Please cite this article in press as: Molina-Aiz, F.D. et al., A study of natural ventilation in an Almería-type greenhouse with insect screens by means of tri-sonic anemometry, Biosystems Engineering (2009), doi:10.1016/j.biosystemseng.2009.06.013

ventilation flow rate for each vent opening has been calculated by measuring air velocity through the openings. We have determined the wind effect coefficient C_w and the discharge coefficient due to the presence of the insect-proof screens in the greenhouse vents C_d. This study differs from previous ones since it attempts to estimate the coefficients C_w and C_d that characterise the ventilation flow through a greenhouse, based on direct measurements of inflow and outflow through ventilation openings by tri-sonic anemometers and based on wind-tunnel experiments, respectively.

2. Materials and methods

2.1. Greenhouse characteristics and location

The Almería-type greenhouse used for the present study consists of a «*raspa y amagado*» structure, the most common type in this province, and is located on the Almería University Campus (latitude: 36°50′, longitude: 2°23′). The NW–SE oriented experimental greenhouse is a 4770 m^3 five-span Almería-type greenhouse (Fig. 1). All openings are manually operated and are covered with insect-proof screens of 10×20 threads cm^{-2} (0.34 porosity; 233.0 μm pore width; 741.3 μm pore height; 271.9 μm thread diameter). Measurements were taken on 4th, 11th, 13th and 15th February 2008, between 11:00 h and 18:45 h (local time, GMT + 1 h) when the outside climatic conditions were stable (Table 1). The Almería province is characterised by two frequent winds channelled by the Mediterranean basin: the *Levante*, a warm dry northeast wind blowing from the land to the sea and the *Poniente*, a cold damp westerly wind (Kuciauskas *et al.*, 1998). However, in the particular case of our experimental greenhouse (located 10 m from the sea), both winds are cold as they blow parallel to the beach. These winds provide remarkable conditions for wind research, because of their frequency, constancy of direction and persistence (Table 1). The greenhouse contained a tomato crop (*Solanum lycopersicum L.* cv. Pitenza) with an average height of approximately 2 m during the period of measurement and a leaf area index of about 1.6 m^2 leaf per m^2 ground.

2.2. Measuring equipment

Temperature and humidity inside the greenhouse were registered as the average of three sensors placed 1.5 m above the soil, below the ridges of the three central spans. Internal air temperature and relative humidity were measured every 2 s by means of a HOBO® Pro Temp-HR U23-001 data logger (Onset Computer Corp., Pocasset, USA), equipped with temperature and humidity probes. This measured the temperature in a range of −20 °C to 70 °C with accuracy of ±0.18 °C and the relative humidity from 0% to 100% with an accuracy of ±2.5%. Temperature sensors were protected against direct solar radiation with a passive solar radiation open shield.

Outside climatic conditions were measured using a portable meteorological station located 2 m from the southwest side wall at a height of 4 m (Fig. 1). Outside temperature and humidity were measured by a HOBO® Pro RH-Temp H08-032-08. Solar radiation was measured with a LI-200SA pyranometer sensor (Li-Cor Inc., Lincoln, USA). This photovoltaic-based sensor covers a limited spectral range (400–1100 nm) with an accuracy of ±5%. The outside wind speed was recorded by means of a cup anemometer (Davis Instrument Corp., Hayward, USA), with a measurement range of 0–78 $m\,s^{-1}$, an accuracy of ±5% and a resolution of 0.09 $m\,s^{-1}$. The wind direction was measured with a vane (accuracy ±7° and resolution 1.4°). These three sensors were connected to a data logger HOBO® H08-006-04 for data recording.

The three components of air velocity in the greenhouse openings were measured by means of a 3D sonic anemometer (model CSAT3, Campbell Scientific Spain S.L., Spain; resolution: 0.001 $m\,s^{-1}$; accuracy ±0.04 $m\,s^{-1}$; vertical path length: 5.8 cm, measurement rate: up to 60 Hz). Data were recorded by a Micrologger CR3000 (Campbell Scientific Spain S.L., Spain). Turbulence intensity on the axis perpendicular to the side

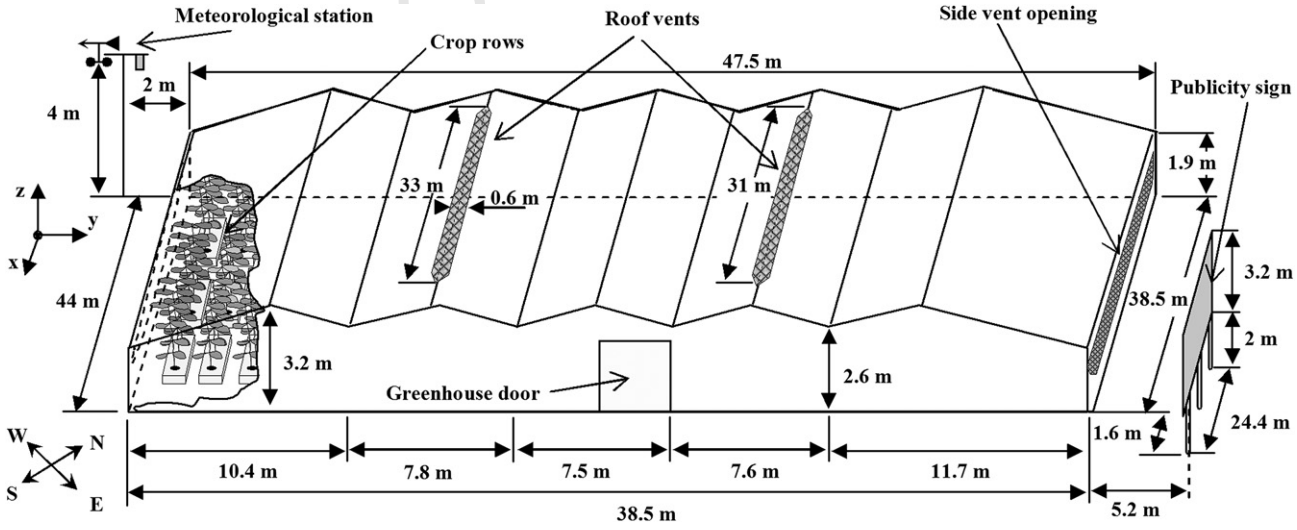

Fig. 1 – Schematic view of the Almería-type greenhouse with the plant rows.

Please cite this article in press as: Molina-Aiz, F.D. et al., A study of natural ventilation in an Almería-type greenhouse with insect screens by means of tri-sonic anemometry, Biosystems Engineering (2009), doi:10.1016/j.biosystemseng.2009.06.013

Table 1 – Climatic conditions recorded both inside and outside the greenhouse during the 4 measurement periods (average ± standard deviation)

Date	Local time	U_o, m s^{-1}	θ, °[a]	T_o, °C	T_i, °C	$U_o/\Delta T_{io}^{0.5}$	HR_o, %	HR_i, %	R_g, W m^{-2}
4/2/08	11:45–18:45	3.89 ± 1.41	212 ± 22 SW	18.3 ± 1.1	23.0 ± 2.5	1.80	62 ± 6	63 ± 7	289 ± 152
15/2/08	10:45–14:45	3.34 ± 1.21	248 ± 21 SW	17.9 ± 0.5	25.3 ± 1.6	1.23	51 ± 3	56 ± 7	395 ± 77
11/2/08	11:15–15:00	8.40 ± 2.00	72 ± 14 NE	15.7 ± 0.5	20.9 ± 1.4	3.67	47 ± 2	47 ± 3	369 ± 62
13/2/08	11:00–15:00	7.19 ± 2.13	55 ± 15 NE	16.1 ± 0.5	20.1 ± 1.5	3.56	43 ± 3	48 ± 3	333 ± 94

Wind speed U_o, wind direction θ, outside temperature T_o, inside temperature T_i, ratio determining the relative importance of the wind and thermal buoyancy forces $U_o/\Delta T_{io}^{0.5}$, outside humidity HR_o, inside humidity HR_i and outside radiation R_g.
a Direction perpendicular to the windows is 66° for a *Levante* wind from northeast (NE) and 232° for a *Poniente* wind from southwest (SW).

vent openings was calculated as the standard deviation divided by the mean local velocity measured by the anemometer $i_y = \sigma_{uy}/u_y$ ($i_z = \sigma_{uz}/u_z$ for the roof vents).

In each of the side openings air velocity was measured in three central profiles (B, C and D in Fig. 2) at four different heights (1, 2, 3 and 4 in Fig. 3a) and two side profiles (A and E in Fig. 2) at the upper two heights, while in the roof vents measurements were taken at three profiles at two different points (Figs. 3b and 2b). More points were used in the side openings, because they have a less uniform shape (Fig. 2), whereas the roof vents have a rectangular shape (Fig. 1). We have calculated the average volumetric flow rate through the openings by multiplying the average air velocity normal to the plane of the opening at each point by the corresponding area. The mean surface corresponding to each point is 2.1 m^2. This value is similar to that used by Boulard *et al.* (1998) to calculate the ventilation flux throughout the only roof vent of a tunnel greenhouse (2.6 m^2 per point) and between those used by Teitel *et al.* (2008) in a monospan greenhouse with two side vent openings (1.1 m^2 per point) and by the same authors (Teitel *et al.*, 2005) in a four-span greenhouse with three roof vents (8.5 m^2 per point). At each point the sonic anemometer measured at a sampling rate of 10 Hz for 3 min (6 min for the first test on 4/2/2009).

2.3. *Ventilation models*

The main driving forces of ventilation for a greenhouse equipped with both roof and side openings are caused by a combination of pressure differences induced by the following effects (Boulard and Baille, 1995; Kittas *et al.*, 1997; Baptista *et al.*, 1999):

- The static wind effect due to the mean component of the wind velocity, which induces pressure differences (side wall effect) between the side and the roof openings (Bruce, 1978) and pressure differences between the windward and the leeward parts of the greenhouse (Boulard *et al.*, 1996).
- The buoyancy forces (also called stack or chimney effect) generating a vertical distribution of pressures between the side and roof openings (Bruce, 1982).
- The turbulent effect of the wind, generated by pressure fluctuations of the wind velocity along and across the greenhouse openings (Boulard and Baille, 1995; Boulard *et al.*, 1996).

These effects generate a vertical ventilation flux due to the chimney effect and the vertical wind pressure distribution (mean and turbulent), and a horizontal ventilation flux due to the side wall and the turbulent effects (Kittas *et al.*, 1997). As a simplification of these effects, we can consider that greenhouse ventilation is the combined result of two fluxes generated by wind and buoyancy forces. We can combine these fluxes obtaining different models derived from Bernoulli's equation (Boulard and Baille, 1995; Boulard *et al.*, 1997a; Kittas *et al.*, 1997):

(1) *Model 1*. In this model the flow is driven by the pressure field equal to the sum of the two independent pressure

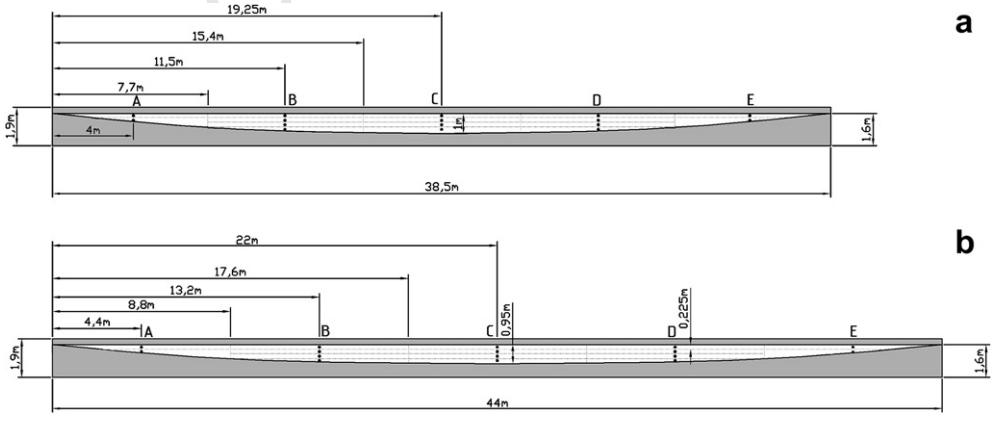

Fig. 2 – Location of anemometers for airspeed measurements in the northeast (a) and southwest side openings (b) with division of each elementary surface S_{vj} (thin broken line).

Please cite this article in press as: Molina-Aiz, F.D. et al., A study of natural ventilation in an Almería-type greenhouse with insect screens by means of tri-sonic anemometry, Biosystems Engineering (2009), doi:10.1016/j.biosystemseng.2009.06.013

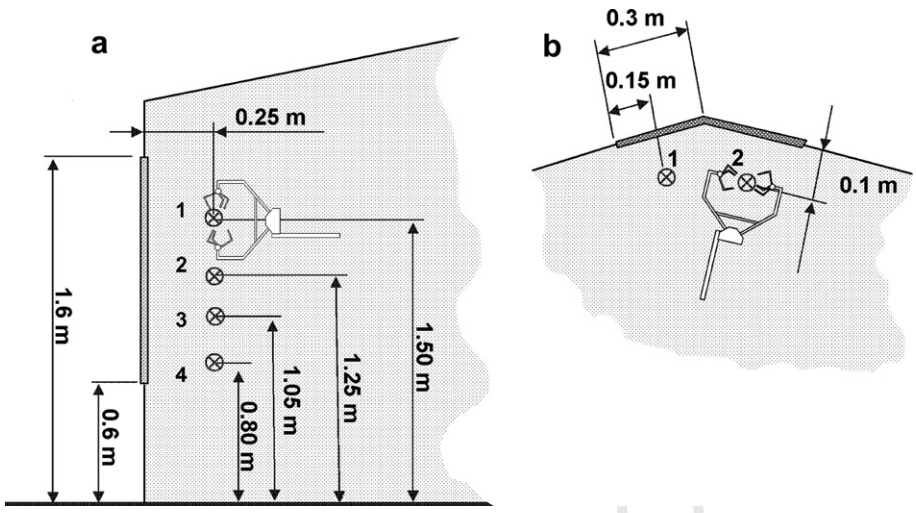

Fig. 3 – Location of sonic anemometer in the side openings (a) and roof vents (b).

fields (Zhang *et al.*, 1989). Therefore, for a greenhouse equipped with side and roof openings, G is calculated as the vector sum of the free component of the ventilation flux induced by buoyancy forces G_T, and the forced component of the ventilation flux induced by wind forces G_w, $G = \sqrt{G_T^2 + G_w^2}$ (Kittas *et al.*, 1997):

$$G = C_d \sqrt{\left(\frac{S_{VR}S_{VS}}{\sqrt{S_{VR}^2 + S_{VS}^2}}\right)^2 \left(2g\frac{\Delta T_{io}}{T_o}h_{SR}\right) + \left(\frac{S_{VR} + S_{VS}}{2}\right)^2 C_w U_o^2} \quad (1)$$

where S_{VR} and S_{VS} are the sum of the two roof and the two side openings' surface areas, respectively, in m^2, g is the gravitational constant in $m\,s^{-2}$, ΔT_{io} is the outside–inside temperature gradient in K, T_o is the outside temperature in K, U_o is the wind speed, C_d is the discharge coefficient, C_w is the wind effect coefficient and h_{SR} is the vertical distance between the midpoint of side and roof openings, in m.

(2) *Model 2*. We consider that the resulting flux is the sum of two independent fluxes, calculating the greenhouse volumetric flow rate as the algebraic sum of the air fluxes, $G = G_T + G_w$ (Boulard and Baille, 1995; Kittas *et al.*, 1997):

$$G = C_d \left[\frac{S_{VR}S_{VS}}{\sqrt{S_{VR}^2 + S_{VS}^2}}\sqrt{2g\frac{\Delta T_{io}}{T_o}h_{SR}} + \frac{S_{VR} + S_{VS}}{2}\sqrt{C_w}U_o\right] \quad (2)$$

(3) *Model 3*. The simplest model only takes into consideration the wind effect. This model is appropriate for high wind speed, when the contribution of stack effect is negligible and the ventilation rate can be calculated as (Boulard and Baille, 1995; Kittas *et al.*, 1996)

$$G = \frac{S_{VR} + S_{VS}}{2}C_d\sqrt{C_w}U_o \quad (3)$$

2.4. *Anemometric measurement of volumetric flow rate*

In order to obtain sufficiently accurate data, wind must remain constant in both direction and strength for 4 or 5 h. Four tests were carried out at around noon, when the wind tends to be stronger and to maintain a more constant direction (Fig. 4). Table 1 shows the mean outside wind direction was 55–72° and 212–248° for the cases of *Levante* and *Poniente* wind, respectively. It can be seen that for two cases the southwest wind direction was approximately perpendicular to the southwest side vent opening (232° SW), and for the other two tests the northeast wind blowing ranged around the direction perpendicular to the other side vent opening and the two roof vents (66° NE).

The mean and turbulent volumetric flow rates through the greenhouse were calculated by multiplying the scaled mean $\overline{u_j}$ and turbulent u' components of the air velocity perpendicular to the plane of the opening to the elementary surface S_{Vj} (Fig. 2) in order to describe the air circulation through the opening (Boulard *et al.*, 1998)

$$\overline{G_j} = \sum_{j=1}^{n} S_{Vj}\overline{u_j} \quad (4)$$

$$G'_j = \sum_{j=1}^{n} S_{Vj}u'_j \quad (5)$$

With only one sampling position possible at any one time, a difficulty arises from how to deal with changing external conditions throughout the time needed to measure the 44 different measurement positions (Figs. 2 and 3). This problem can be overcome by selecting measurements for a fixed external wind direction and correcting the air velocities measured by the 3D sonic anemometer at each position j at the greenhouse openings $u_j(t)$ through a process of scaling with the wind speed (Appendix A). However, we have also used a second procedure scaling the air velocities measured by the 3D sonic anemometer by the inverse of the normalised ventilation flux $G(t)/\overline{G}$, as given below:

$$u_j^*(t) = u_j(t)\frac{\overline{G}}{G(t)} \quad (6)$$

The inverse of the normalised ventilation flux used in Eq. (6) was calculated as the ratio of the mean volumetric flow rate

Please cite this article in press as: Molina-Aiz, F.D. et al., A study of natural ventilation in an Almería-type greenhouse with insect screens by means of tri-sonic anemometry, Biosystems Engineering (2009), doi:10.1016/j.biosystemseng.2009.06.013

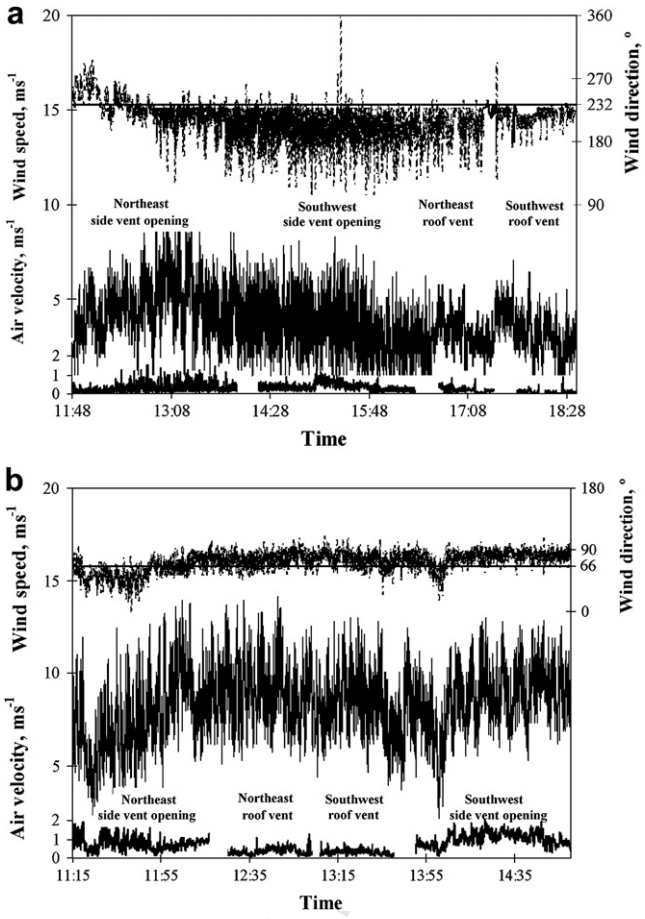

Fig. 4 – Evolution of air velocity through the vent openings (—) and the outside wind speed (—) and direction (–·–) for the measurements made on 4/2/2008 with a southwest Poniente wind (a), and on 11/2/08 with a northeast Levante wind (b).

$\overline{G} = G(\overline{\Delta T_{io}}, \overline{T_o}, \overline{U_o})$ to the instantaneous volumetric flow rate $G(t) = G[\Delta T_{io}(t), T_o(t), U_o(t)]$. $\overline{G}$ was calculated with Eq. (2) using the average values of the climatic parameters ($\overline{T_o}$, $\overline{\Delta T_{io}}$ and $\overline{U_o}$) for the whole measurement period (several hours), whereas $G(t)$ was calculated with climatic parameters averaged over the measurement period t (each minute) at position j [$T_o(t)$, $\Delta T_{io}(t)$, $U_o(t)$]. A detailed expression of the normalisation formula is given in Appendix B.

The use of Eq. (6) is based on the assumption that the variations of mean air velocity through the greenhouse openings over time are proportional to the variations in the ventilation volumetric flow rate, and considering these variations to be produced both by variations in the outside wind speed (Fig. 4) and by variations in the temperatures inside and outside the greenhouse (Fig. 5).

2.5. *Discharge coefficient of the insect-proof screen*

The analysis of the aerodynamic characteristics of the greenhouse screen, and the respective discharge coefficient, was carried out with wind-tunnel experiments providing data of the pressure drop as a function of air velocity. A detailed description of the wind-tunnel experiment was provided by Valera *et al.* (2006) and details of the wind-tunnel instrumentation were presented by Molina-Aiz *et al.* (2006).

The airflow through a porous mesh (very porous medium) can be described by a modification of Darcy's equation (Forchheimer, 1901):

$$\frac{\partial p}{\partial x} = -\left(\frac{\mu}{K_p}u + \rho\left(\frac{Y}{K_p^{1/2}}\right)|u|u\right) \quad (7)$$

where P is the pressure in Pa, x the direction of flow, K_p is a coefficient independent of the nature of the fluid which depends on the geometry of the medium. It has dimensions (length)^2 and is called the specific permeability of the medium (Nield and Bejan, 1999). Y is a dimensionless form-drag constant dependent on the nature of the porous medium, called inertial factor. According to Forchheimer's equation, a second-order polynomial (Miguel *et al.*, 1997; Dierickx, 1998; Muñoz *et al.*, 1999) has been used for fitting the experimental values of pressure drop an air velocity measured in a wind tunnel (Valera *et al.*, 2006; Molina-Aiz *et al.*, 2006) through the screen:

$$\Delta P = -(au^2 + bu + c) \quad (8)$$

The best fit equation $\Delta P = -(2.190u^2 + 2.885u - 0.621)$ obtained from the wind-tunnel experiment provides the values of coefficients $a = 2.190$ and $b = 2.885$ [zero order term can be neglected compared with the other terms (Miguel *et al.*, 1997)]. Equating the first- and second-order terms,

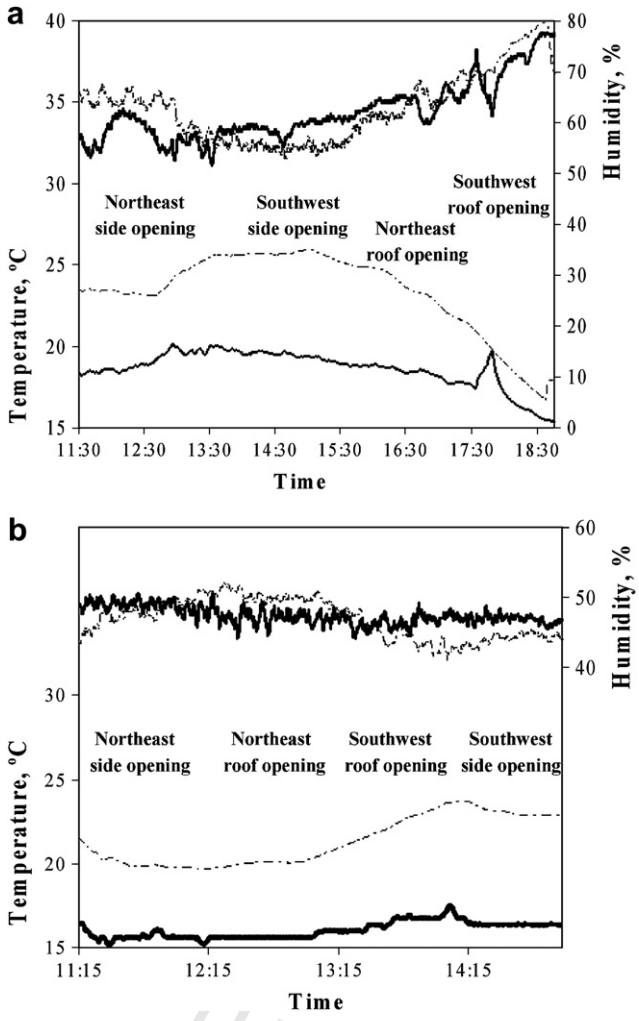

Fig. 5 – Temperature and relative humidity variations with time for the measurements made on 4/2/2008 with a southwest Poniente wind (a), and on 11/2/08 with a northeast Levante wind (b). Values outside the greenhouse (thick continuous line) and inside the greenhouse (thin dotted lines).

Table 2 – Average values of the mean normalised air velocity $\overline{u}/U_o$ perpendicular to the greenhouse vents registered on 4/2/2008 and on 11/2/2008 (u is positive for an inflow and negative for an outflow)

Vent opening	Northeast (NE) side vent				NE roof vent		SW roof vent		Southwest (SW) side vent			
Height (m)	0.80	1.05	1.25	1.50	0.15	0.45	0.15	0.45	0.80	1.05	1.25	1.50
Measurements taken on 4/2/2008 with a Poniente *wind from southwest*												
Extreme SE			−0.01	−0.03	−0.02	−0.04	−0.03	−0.03			+0.04	+0.04
Middle SE	+0.04	+0.03	+0.02	−0.02					+0.03	+0.04	+0.03	+0.02
Centre	+0.04	+0.06	+0.03	−0.01	−0.01	−0.04	−0.03	−0.04	+0.03	+0.06	+0.05	+0.03
Middle NW	+0.02	+0.03	−0.01	−0.01					+0.06	+0.11	+0.08	+0.11
Extreme NW			+0.01	−0.02	−0.02	−0.02	−0.01	−0.04			+0.04	+0.07
Measurements taken on 11/2/08 with a Levante *wind from northeast*												
Extreme SE			−0.07	−0.08	−0.07	−0.06	−0.06	−0.03			+0.05	+0.06
Middle SE	−0.05	−0.04	−0.04	−0.03					+0.05	+0.08	+0.08	+0.07
Centre	−0.04	−0.02	+0.00	+0.02	−0.06	−0.06	−0.03	−0.02	+0.07	+0.07	+0.07	+0.08
Middle NW	+0.07	+0.12	+0.09	+0.07					+0.03	+0.06	+0.09	+0.07
Extreme NW			+0.07	+0.10	−0.06	−0.05	−0.04	−0.03			+0.03	+0.05

Please cite this article in press as: Molina-Aiz, F.D. et al., A study of natural ventilation in an Almería-type greenhouse with insect screens by means of tri-sonic anemometry, Biosystems Engineering (2009), doi:10.1016/j.biosystemseng.2009.06.013

respectively, of the experimental polynomial [Eq. (8)] and Forchheimer's [Eq. (7)], the permeability and the inertial factor can be obtained:

$$K_p = e\frac{\mu}{b} \tag{9}$$

$$Y = \frac{aK_p^{0.5}}{e\rho} \tag{10}$$

where the thickness of the screen $e = 371.3$ μm was obtained measuring a transversal section of the net with a microscope (Valera *et al.*, 2006). Bernoulli's equation can also be used to describe the relationship between pressure drop and air velocity through the screens (Kosmos *et al.*, 1993; Montero *et al.*, 1997; Teitel and Shklyar, 1998):

$$\Delta P = -1/2F_\varphi \rho u^2 \tag{11}$$

where F_φ is the pressure drop coefficient of the screen. We have calculated this pressure drop coefficient from the wind-tunnel test, making Eq. (7) equal to Eq. (11) with $\partial P/\partial x = \Delta P/e$, giving

$$F_\varphi = \frac{2e}{K_p^{0.5}}\left(\frac{1}{Re_p} + Y\right) \tag{12}$$

This coefficient can be used to predict the pressure drop through screens even at $Re_p < 150$ (Teitel, 2001). The Reynolds number based on the screen's permeability Re_p was calculated considering the average airspeed passing through the 44 points in the openings at the time of measurement. This Reynolds number is calculated for application to porous media considering the square-root of the permeability as a characteristic dimension (Nield and Bejan, 1999):

$$Re_p = \frac{\sqrt{K_p}up}{\mu} \tag{13}$$

The discharge coefficient of the insect-proof screens $C_{d,\varphi}$ has been calculated from the pressure drop coefficient due to the presence of an insect-proof screen F_φ [given by Eq. (12)] as

$$C_{d,\varphi} = 1/F_\varphi^{0.5} \tag{14}$$

2.6. Estimation of pressure drop coefficient of the greenhouse openings

In order to determine the greenhouse's wind effect coefficient it is necessary to know the discharge coefficient of the windows C_d, as well as the surface area of the side and roof vent openings ($S_{VS} = 56.0$ m^2 and $S_{VR} = 38.4$ m^2), the difference in height between windows ($h_{SR} = 2.10$ m), the thermal gradient ΔT_{io}, the wind speed U_o and the outside air temperature T_o (Table 1). The discharge coefficient of the opening C_d has been calculated as follows (Arbel *et al.*, 2000; Kittas *et al.*, 2002):

$$C_d = \sqrt{\frac{1}{\frac{1}{C_{d,LH}^2} + \frac{1}{C_{d,\varphi}^2}}} \tag{15}$$

where $C_{d,LH}$ is the discharge coefficient due to the shape of the window and $C_{d,\varphi}$ is the discharge coefficient of the insect-proof screen given by Eq. (14). The discharge coefficient of the

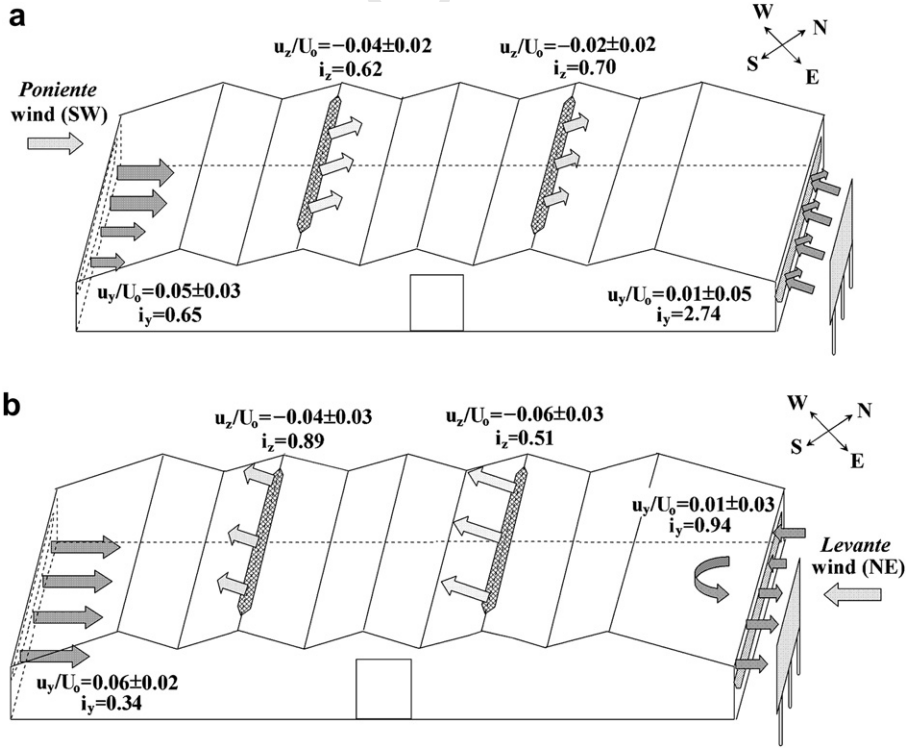

Fig. 6 – Sketch of the airflow pattern in the vent openings of the Almería-type greenhouse for a southwest Poniente wind on 4/2/2008 (a) and for a northeast Levante wind on 11/2/2008 (b), with values of the normalised air velocity perpendicular to the openings and turbulence intensity.

Please cite this article in press as: Molina-Aiz, F.D. et al., A study of natural ventilation in an Almería-type greenhouse with insect screens by means of tri-sonic anemometry, Biosystems Engineering (2009), doi:10.1016/j.biosystemseng.2009.06.013

Table 3 – Values of the mean ventilation volumetric flow rate $\overline{G_j}$ ($m^3 s^{-1}$) through each point of measurement j at the greenhouse openings calculated with values or air velocities $\overline{u_j^*}$ corrected with wind speed and buoyancy forces (Appendix B), for the four tests (G is positive for an inflow and negative for an outflow)

Vent opening	Northeast (NE) side vent				NE roof vent		SW roof vent		Southwest (SW) side vent			
Height (m)	0.80	1.05	1.25	1.50	0.15	0.45	0.15	0.45	0.80	1.05	1.25	1.50
Measurements taken on 4/2/2008 with a Poniente *wind from southwest*												
Extreme SE			−0.06	−0.16	−0.28	−0.44	−0.54	−0.65			+0.27	+0.25
Middle SE	+0.23	+0.18	+0.11	−0.11					+0.18	+0.31	+0.26	+0.20
Centre	+0.40	+0.44	+0.19	−0.08	−0.16	−0.46	−0.38	−0.55	+0.25	+0.35	+0.36	+0.23
Middle NW	+0.12	+0.16	−0.04	−0.07					+0.31	+0.84	+0.68	+0.82
Extreme NW			+0.05	−0.09	−0.23	−0.28	−0.21	−0.59			+0.21	+0.46
Total inflow						+7.86	Total outflow		−5.39	Mean flow		6.63
Measurements taken on 11/2/08 with a Levante *wind from northeast*												
Extreme SE			−0.91	−1.11	−2.09	−1.71	−1.62	−0.83			+0.77	+0.88
Middle SE	−0.61	−0.65	−0.70	−0.43					+0.48	+1.31	+1.28	+1.24
Centre	−0.75	−0.32	+0.07	+0.31	−1.73	−1.84	−0.87	−0.63	+1.29	+1.24	+1.11	+1.34
Middle NW	+0.71	+1.71	+1.22	+0.91					+0.30	+1.01	+1.35	+1.12
Extreme NW			+0.83	+1.19	−1.53	−1.44	−1.03	−0.77			+0.49	+0.77
Total inflow						+22.91	Total outflow		−21.55	Mean flow		22.23
Measurements taken on 13/2/08 with a Levante *wind from northeast*												
Extreme SE			−0.74	−0.79	−1.97	−1.47	−0.21	−0.22			+0.85	+0.79
Middle SE	−0.54	−0.54	−0.60	−0.59					+0.66	+1.24	+1.35	+1.28
Centre	−0.40	−0.02	−0.01	−0.43	−2.20	−0.96	−1.11	−0.40	+1.15	+1.36	+1.44	+1.44
Middle NW	+0.98	−1.32	−1.41	−1.15					+0.26	+1.22	+1.34	+1.21
Extreme NW			+1.32	+1.01	−1.54	−0.78	−0.94	−0.76			+0.56	+1.03
Total inflow						+20.48	Total outflow		−21.10	Mean flow		20.79
Measurements taken on 15/2/2008 with a Poniente *wind from southwest*												
Extreme SE			+0.03	+0.14	−0.31	−0.90	−0.28	−0.92			+0.04	+0.12
Middle SE	+0.35	+0.15	−0.03	−0.08					+0.23	+0.37	+0.09	+0.09
Centre	+0.18	+0.27	−0.10	−0.10	−0.30	−0.85	−0.30	−0.86	+0.37	+0.49	+0.50	+0.19
Middle NW	+0.09	+0.13	+0.05	+0.03					+0.38	+0.58	+0.63	+0.47
Extreme NW			−0.01	+0.03	−0.38	−0.70	−0.27	−0.88			+0.51	+0.68
					Total inflow	+7.19	Total outflow		−7.27	Mean flow		7.23

Please cite this article in press as: Molina-Aiz, F.D. et al., A study of natural ventilation in an Almería-type greenhouse with insect screens by means of tri-sonic anemometry, Biosystems Engineering (2009), doi:10.1016/j.biosystemseng.2009.06.013

openings without screen was calculated as follows (Bailey *et al.*, 2003):

$$C_{d,LH} = \{1.9 + 0.7\exp[-L/(32.5H\sin\alpha)]\}^{-0.5} \quad (16)$$

where L is the length of the window, H the height and α the angle of opening (with a value of $\alpha = 90°$ for an opening without flaps).

3. Results and discussion

3.1. *Measurement of air velocity through the greenhouse openings*

In order to compare the air velocity measured at several positions in the greenhouse openings between the four cases, and since the outside wind varied during the period of measurement (Fig. 4), normalised air velocity values were calculated (Table 2). The normalised components of the air velocity vectors on the axis perpendicular to the greenhouse side and roof (Fig. 1), were calculated as the ratio of the air velocity components measured by the 3D sonic anemometer u_j at each position j in the greenhouse openings to the external wind speed measured during the same time period U_o, i.e. u_y/U_o and u_z/U_o.

The mean values of the normalised component of air velocity ($\overline{u_j}/Uo$) perpendicular to the side vent openings and roof vents are presented in Fig. 6a and b for the cases of *Poniente* and *Levante* winds, respectively. For a weak southwest *Poniente* wind, the spatial distribution of mean velocity was more uniform in the four windows, although in the windward side vents we can observe that air entered mainly through the southeast part of the opening (Table 2), because this part is close to the sea and without obstacles, while the northwest part is close to other greenhouses and buildings. This effect can also be observed in the two roof vents, but in these cases the flow is more uniform. For a strong northeast *Levante* wind, the spatial distribution in the leeward side vent and the two roof vents was very uniform (Table 2). On the other hand, for the windward side vent, airflow entered through the northwest part of the window, directly exposed to the wind (Fig. 6b), whereas air exited through the southeast part where there is a publicity sign 5.2 m upstream from the greenhouse (Fig. 1).

The average value for the four tests of the absolute normalised air velocity ($|u/U_o|$) in the vent openings was 0.037 with a standard deviation of 0.034. These values are close to those measured by Kittas *et al.* (2008) near the side opening in a greenhouse with a curved roof and vertical side walls, equipped with two side roll-up windows and a flap roof window. They obtained normalised air velocities of 0.070 ± 0.015 and 0.039 ± 0.022 for the west and east side openings with screens (265 μm wire diameter, 150×150 μm hole size, and 50% porosity), respectively, whereas the respective values near the two side openings without screens were 0.392 ± 0.050 and 0.138 ± 0.047. The use of insect screens in the ventilation openings resulted in an average decrease of 76% in the normalised air velocity measured near the side vents (Kittas *et al.*, 2008), and

Table 4 – Ventilation volumetric flow rates through each vent openings calculated from Eq. (4) with values of air velocities u^* corrected with wind speed and buoyancy forces (Appendix B): windward side $\overline{G}_{SW}$, leeward side $\overline{G}_{SL}$ windward roof $\overline{G}_{RW}$ and leeward roof $\overline{G}_{RL}$

Date	$\overline{G}_{SW}(u^*)$, $m^3\,s^{-1}$	$\overline{G}_{SL}(u^*)$, $m^3\,s^{-1}$	$\overline{G}_{RW}(u^*)$, $m^3\,s^{-1}$	$\overline{G}_{RL}(u^*)$, $m^3\,s^{-1}$	$\overline{G}_M(u^*)$, $m^3\,s^{-1}$	$\frac{\Delta G(u^*)}{\overline{G}_M(u^*)}$, %	$\frac{\Delta G(\overline{u})}{\overline{G}_M(\overline{u})}$, %	$\frac{\Delta G(u)}{\overline{G}_M(u)}$, %	G', $m^3\,s^{-1}$	A	B	C
4/2/08	+5.99	+1.87–0.62	−2.91	−1.86	6.63	+37.3	+45.9	+70.5	5.50	4.80	41.2	0.70
15/2/08	+5.73	+1.46–0.30	−3.52	−3.45	7.23	−1.2	+6.7	+10.5	4.94	5.22	41.2	0.56
11/2/08	+6.94–5.47	+15.97	−10.32	−5.75	22.23	+6.1	+11.0	+8.4	10.22	7.27	41.2	1.90
13/2/08	+4.23–7.63	+17.17	−8.91	−3.64	20.79	−3.0	+8.7	+25.8	12.66	7.13	41.2	2.14

Difference $\Delta\overline{G}$ between the mean volumetric flow rate entering through the vents (positive values) and that which exits (negative values) expressed as a percentage of the average mean volumetric flow rate $\overline{G}_M$: calculated from u^* (Appendix B), from air velocities $\overline{u}$ scaled with only outside wind speed (Appendix A) and from air velocities u without corrections. Turbulent component of the volumetric flow rate G' [from Eq. (5)] and values of the three parameters A, B and C used in Appendix B.

therefore a reduction of the wind-induced greenhouse ventilation rate. The calculated values of normalised air velocity for the side openings, ranging between 0.01 and 0.08, are lower than those obtained by Katsoulas *et al.* (2006), who recorded 0.24 for the windward vent, but similar to the value the same authors measured in the leeward vent ($u/U_o = 0.07$) in a mono-span greenhouse with screens of 50% porosity.

The airflow pattern for a *Poniente* wind was similar in the two cases studied, with air entering the greenhouse *via* the windward side vent and the lower part of the leeward side vent (Table 2) and exiting through the roof vents and the upper part of the leeward side opening (Fig. 6a). This result is qualitatively in good agreement with the airflow patterns simulated with CFD and measured with an omnidirectional anemometer (Molina-Aiz *et al.*, 2004b) inside the same greenhouse with two side openings and with only one roof vent placed in the central ridge, for *Poniente* wind. However, when the greenhouse was equipped with only one central roof vent, the leeward side opening acted as the entrance for outside air, whereas when there were two roof vents, the upper part of the leeward side opening acted as the exit for air (Fig. 6a). The side vent was particularly important for enhancing the air exchange rate between the inside and outside (Bournet *et al.*, 2007).

On the other hand, a *Levante* wind blowing perpendicular to the greenhouse ridge produces an outflow through the half of the northeast side vent opening close to the obstacle (an advertising sign), whereas in the other half of this side opening, the air enters the greenhouse. The normal flow to the frontal face of an obstacle (such as the advertising sign) creates a negative pressure zone on its leeward face (Baetke *et al.*, 1990), and when the obstacle is close to a plane (the ground) a recirculation region forms downstream (Bhattacharyya and Maiti, 2004). This negative pressure zone with air recirculation produces an outflow through the half of the northeast side opening next to the advertising sign. For this *Levante* wind, we can also observe an inflow at the southwest side opening (free of obstacles) and an outflow at the roof vents, where wind produces suction (Simiu and Scanlan, 1996). At the northeast side opening, influenced by the proximity of obstacles to the greenhouse, the airflow depends on the wind direction, whereas the behaviour of the southwest side and the roof openings was independent of the wind direction, acting as entrance and exits of air, respectively.

Table 5 – Values corresponding to the Reynolds number based on the permeability of the screen Re_p and the average speed of air circulation in the windward vent, pressure-loss coefficient due to the presence of the insect-proof screen F_φ, discharge coefficient corresponding to the effect of the screen $C_{d,\varphi}$, discharge coefficient according to the vent geometry $C_{d,LH}$ and total discharge coefficient of the vent opening C_d

Date	Re_p	F_φ	$C_{d,\varphi}$	$C_{d,LH}$	C_d
4/2/08	0.41	41.20	0.156	0.696	0.152
15/2/08	0.50	34.37	0.171	0.696	0.166
11/2/08	1.18	16.62	0.245	0.696	0.230
13/2/08	1.12	17.38	0.240	0.696	0.227

3.2. *Evaluation of the mean and turbulent ventilation flows*

The precision of the average air exchange measurements can be checked by summing inflows and outflows over the whole openings surface in order to verify the degree to which the mass conservation in the greenhouse is satisfied (Boulard *et al.*, 1997b). The mean ventilation flux $G(u^*)$ (Table 3) has been calculated from Eq. (4) using velocities scaled with the inside–outside differences in temperature and wind speed $[u(t)\overline{G}/G(t)]$ (Appendix B) reducing the average difference between outflow and inflow to +9.8% (Table 4). This difference was +18.1% for the values of $G(\ddot{u})$ calculated scaling the air velocity only with the wind speed $[u(t)\overline{U_o}/U_o(t)]$ (Appendix A), and was +28.8% for the ventilation flux $G(u)$ calculated with the velocities measured directly with the anemometer without scaling $[u(t)]$.

The greenhouse ventilation rate is affected by the buoyancy effect generated by the average characteristic temperature difference between the inside and the outside air ΔT_{io}. Papadakis *et al.* (1996) showed that the effect of buoyancy on greenhouse ventilation could not be neglected at wind speeds lower than about 1.8 m s^{-1}. In greenhouses with both roof and side openings, Kittas *et al.* (1997) considered that the stack effect is important if the ratio $U_o/\Delta T_{io}^{0.5} < 1$. In our case, the mean values of $U_o/\Delta T_{io}^{0.5}$ during the period of measurement were 1.52 m s^{-1} K$^{-0.5}$ for the weak *Poniente* wind and 3.62 m s^{-1} K$^{-0.5}$ for the strong *Levante* wind, respectively (Table 1). *A priori*, for all cases studied the stack effect can be neglected. However, for the second test with the *Poniente* wind (15/02/08) the ratio $U_o/\Delta T_{io}^{0.5} = 1.23 \pm 0.30$ was smaller, and during a significant part of the measurement period it was lower than the threshold ratio of 1 m s^{-1} K$^{-0.5}$. This suggests that the buoyancy effect could have been important, as Katsoulas *et al.* (2006) found for a greenhouse with roof and side openings.

Buoyancy effects not only influence ventilation quantitatively, but also from a qualitative point of view, affecting the form in which air moves inside the greenhouse. There are two fundamentally different modes of buoyancy-driven natural ventilation: displacement and mixing. Displacement ventilation occurs in greenhouses with side and roof vents. Outside air enters through low-level openings and displaces warm air through openings at higher levels (Haslavsky *et al.*, 2006). Thus inflow and outflow are separate and take place through the side and roof vents, respectively. The neutral plane, defined as the vertical level where the internal and outside pressures are equal, is located between the side and roof vents. On the other hand, mixing ventilation occurs when only one roof vent is opened so that inflow and outflow take place through different regions of the same opening. The plume of the incoming cool outside air mixes with the fluid within the space, while warmer air leaves the greenhouse through the upper region of the same roof vent. In mixing ventilation, the neutral plane is approximately at mid-height of the roof vent, separating inflow from outflow (Fitzgerald and Woods, 2007). The ratio between surface areas of the roof vent openings S_{VR} and side vent openings S_{VS} affects the efficiency of the buoyancy ventilation flux (Kittas *et al.*, 1997). In our case the value

Please cite this article in press as: Molina-Aiz, F.D. et al., A study of natural ventilation in an Almería-type greenhouse with insect screens by means of tri-sonic anemometry, Biosystems Engineering (2009), doi:10.1016/j.biosystemseng.2009.06.013

of the S_{VR}/S_{VS} ratio was 0.67. According to Kittas *et al.* (1997), this is in the appropriate range for maximization of the buoyancy ventilation flux ($0.5 < S_{VR}/S_{VS} < 2$). This value is also in the range $0.5 < S_{VR}/S_{VS} < 1$, where the displacement mode of buoyancy-driven natural ventilation prevails and cold outside air enters through low-level openings and displaces warm air from the greenhouse through openings at higher levels (Haslavsky *et al.*, 2006).

Mass conservation is slightly less well satisfied for the first set of measurements (4/2/2008), with a difference of +37.3%, than in the following three studies, where differences ranged between −1.2% and +6.1% (Table 4). For this first test we measured for 6 min on each point, extending the total length of the experimentation to 7 h. This duration implies a greater variation of the outside wind speed (Fig. 4a) and of the temperature difference between inside and outside the greenhouse (Fig. 5a). Fig. 5a shows important differences in the outside–inside temperature gradient for the different measurement locations. When the temperature gradient is greater, at the side vent openings for the test carried out on 4/2/2008 (Fig. 5a), the buoyancy effect is higher, whereas when the temperature gradient drops, the thermal effect on ventilation decreases. These variations of the buoyancy effect are influential in obtaining values of the total inflow in the greenhouse greater than the outflow (Table 4). By calculating the mean ventilation flux $G_M(u^*)$ from velocities scaled with the inside–outside differences in temperature and wind speed (Appendix B), we can partly correct this distortion produced by temperature variations (Table 4).

The differences in inflow–outflow ranged from 31.6% obtained with a tri-sonic anemometer by Boulard *et al.* (1997b) to 2.5% measured with a one-dimensional sonic anemometer by Boulard *et al.* (1996) in a two-span greenhouse with only one roof vent. As expected, the differences in the present study were considerable because the covering structure of the Almería-type greenhouse is held in place by two networks of wires, requiring the plastic to be pierced every metre in order to be held firmly in place. This means that airflow through the holes in the greenhouse cover can lead to significant differences between inflow and outflow through the vent openings. In general, the results obtained with the flows scaled with temperatures and wind speed, indicate that we were able to successfully identify the mean wind component using a tri-sonic anemometer.

The turbulence intensity was on average about 3–9 times larger at the windward side opening than near the leeward opening for the two tests with *Levante* wind (Fig. 6b). Teitel *et al.* (2008) obtained turbulence intensity values about 5 times greater on the windward opening than on the leeward opening. Boulard *et al.* (2000) also showed that the turbulent kinetic energy is greater near the windward than the leeward opening for a tunnel with discontinuous openings and wind blowing perpendicular to the axis of the tunnel. However, for a *Poniente* wind the turbulence intensity was 5 times smaller at the windward side opening (Fig. 6a). It seems that the publicity sign close to the northeast side vents of the experimental greenhouse (Fig. 1) produced an increase in turbulence intensity at the opening for a northeast *Levante* wind when placed in a windward position. The sign generates suction, causing an

Table 6 – Values of the wind effect coefficient C_w and the coefficient of effectiveness of the windows $E_V = C_d C^{0.5}$ for the three ventilation models studied (*M*) obtained by several authors in different greenhouse types with side and roof openings with and without insect-proof screens

Model	C_w	$E_V = C_d C_w^{0.5}$	C_d	Greenhouse type	S_c, m^2	U_o, m s^{-1}	Source
Greenhouse without screen							
M1	0.002	0.025	0.656	Almería	881	2–10	Pérez Parra *et al.*, 2004
M1	0.079	0.210	0.745	Multispan	416	0–8	Papadakis *et al.*, 1996
M1	0.09	0.204	0.68	Multispan	416	0–8	Kittas *et al.*, 1997
M1	0.098	0.175	0.56	Multispan	242	1–3	Sase *et al.*, 2002
M1	0.103[a]	0.210	–	Multispan	179	0.5–2.7	Abreu *et al.*, 2006
M1	0.116	0.303	0.89	Multispan	242	1–3	Sase *et al.*, 2002
M1	0.12	0.208	0.6	Multispan	416	2	Kittas *et al.*, 1996
M1	0.13	0.252	0.7	Multispan	416	0–8	Kittas *et al.*, 1997
M2	0.18	0.178	0.42	Multispan	416	0–8	Kittas *et al.*, 1997
M3	0.012[a]	0.07–0.18	–	Tunnel	240	1–2	Boulard *et al.*, 1997a
M3	0.04[a]	0.13	–	Tunnel	504	2.8	Sbita *et al.*, 1996
M3	0.041[a]	0.131	–	Tunnel	368	5	Fatnassi *et al.*, 2004
M3	0.074	0.178	0.656	Almería	881	2–10	Pérez Parra *et al.*, 2004
M3	0.085[a]	0.19	–	Multispan	416	5.3	Boulard *et al.*, 1997a
M3	0.173[a]	0.27	–	Multispan	10 000	2–4	Demrati *et al.*, 2001

M	φ	C_w	$C_d C_w^{0.5}$	C_d	Greenhouse type	S_c, m^2	U_o, m s^{-1}	Source
Greenhouse with insect-proof screen								
M3	0.5	0.022[a]	0.096	–	Multispan[b]	160	2.2	Katsoulas *et al.*, 2006
M3	0.62	0.071	0.069	0.253	Monospan	74.4	4.5	Teitel *et al.*, 2008
M3	0.69	0.11	0.14	0.42	Canary[a]	5600	1–2	Fatnassi *et al.*, 2002

C_d discharge coefficient of the openings; φ insect-proof screen porosity; S_c greenhouse area; U_o wind speed.
a Wind effect coefficient C_w calculated from coefficient of effectiveness of the windows using $C_d = 0.65$ (discharge coefficients not supplied by the author).

Please cite this article in press as: Molina-Aiz, F.D. et al., A study of natural ventilation in an Almería-type greenhouse with insect screens by means of tri-sonic anemometry, Biosystems Engineering (2009), doi:10.1016/j.biosystemseng.2009.06.013

Table 7 – Discharge coefficients C_d of screened openings analysed in several ventilation studies in greenhouses ordered by the insect-proof screen porosity φ. Geometric characteristics of the insect-proof screens: *D* pore height; *W* pore width; *d* wire diameter; $C_{d,LH}$ discharge coefficient due to the shape of the opening; $C_{d,\varphi}$ discharge coefficient of the insect-proof screens

C_d	$C_{d,LH}$	$C_{d,\varphi}$	φ	Screens	Density[a]	*D*, mm	W, mm	*d*, mm	Source
0.369	0.769	0.42[d]	0.25	Anti-thrip	28 × 28	0.18	0.18	0.18	Montero *et al.*, 1997
0.16[d]	0.65[e]	0.16	0.25	Anti-thrip	29 × 29	0.17	0.17	0.17	Bailey *et al.*, 2003
0.21	0.65[e]	0.22[d]	0.3	78 mesh	21 × 27	0.29	0.18	0.19	Harmanto *et al.*, 2006
0.199	0.707	0.21[d]	0.355	50 mesh	10 × 19	0.26[c]	0.73[c]	0.255	Teitel *et al.*, 1999
0.31[d]	0.65[e]	0.35	0.355	50 mesh	10 × 19	0.26[b]	0.73[c]	0.255	Teitel, 2001
0.28	0.65[e]	0.31[d]	0.38	52 mesh	9 × 18	0.8	0.25	0.31	Harmanto *et al.*, 2006
0.41	0.645	0.53[d]	0.39	Anti-insect	13 × 13	0.47[c]	0.47[c]	0.28	Pérez Parra *et al.*, 2004
0.31	0.65[e]	0.35[d]	0.41	40 mesh	15 × 16	0.44	0.39	0.245	Harmanto *et al.*, 2006
0.51	0.65[e]	0.82[d]	0.45	Anti-aphid	17 × 17	0.40[c]	0.40[c]	0.2	Muñoz *et al.*, 1999
0.509	0.769	0.68[d]	0.45	Anti-aphid	17 × 17	0.40	0.40	0.2	Montero *et al.*, 1997
0.34[d]	0.65[e]	0.41	0.45	Anti-aphid	17 × 17	0.4	0.4	0.2	Bailey *et al.*, 2003
0.40[d]	0.65[e]	0.50	0.53	Anti-insect	21 × 21	0.31	0.31	0.16	Bailey *et al.*, 2003
0.50[d]	0.65[e]	0.80	0.629	17 mesh	6 × 6	1.34[c]	1.34[c]	0.35	Teitel, 2001
0.253	0.66	0.275	0.62	17 mesh	6 × 6	1.406	1.164	0.356	Teitel *et al.*, 2008
0.48[d]	0.65[e]	0.71	0.66	Anti-insect	19 × 19	0.44	0.44	0.1	Bailey *et al.*, 2003
0.49[d]	0.65[e]	0.75	0.68	Anti-insect	18 × 18	0.45	0.45	0.1	Bailey *et al.*, 2003
0.42	0.707	0.52[d]	0.69	36 mesh cm^{-2}	17 × 17	0.50	0.50	0.1	Fatnassi *et al.*, 2002

a Calculated as 10 mm/(*D* + *d*) × 10 mm/(*W* + *d*).
b Obtained from Teitel and Shklyar (1998).
c Estimated values from porosity as $\varphi = DW/[(D + d)(W + d)]$.
d Calculated from Eq. (15).
e Discharge coefficients not supplied by the author (supposes as a rectangular window $C_d = 0.65$).

outflow in the half of the window next to the obstacle, whereas in the other half of this windward side opening, the air enters the greenhouse (Fig. 6b). For a *Poniente* wind blowing from Southwest, at the window close to the publicity sign on the leeward side of the greenhouse, air enters through the lower part of the opening and exits through the upper part (Table 3). In this case the turbulence intensity is also greater than in the southwest side opening, which is free of obstacles.

Local estimations of mean and turbulent flux of sensible energy across a vent opening can be obtained using eddy correlation techniques (Boulard *et al.*, 1996). We have evaluated the turbulent sensible heat exchange by integrating the lateral flux (perpendicular to the vent opening surface) along the opening (Molina-Aiz *et al.*, 2009). The mean flow of sensible heat is estimated at between 86% and 97% of the total flux, and so the turbulent flow does not exceed 14%. The contribution of the turbulent flux was less here, when the wind blows perpendicular to the opening, than the 23–45% obtained by Boulard *et al.* (1996) in a roof vent for a wind parallel to the greenhouse ridge.

3.3. *Evaluation of the discharge coefficients of the greenhouse openings*

Table 5 shows the total discharge coefficients calculated from Eq. (15) for the four dates on which air velocity and average ventilation volumetric flow rates were measured in the experimental greenhouse. The discharge coefficient due to the shape of the openings for the greenhouse $C_{d,LH} = 0.696$ (Table 5) was calculated as an average of values obtained from Eq. (16) for the side ($C_{d,LH} = 0.691$) and the roof openings ($C_{d,LH} = 0.701$). The discharge coefficient due to the shape of the openings $C_{d,LH}$ is equivalent to the total discharge coefficient C_d of an unscreened opening [as we can deduce from Eq. (15) with $C_{d,\varphi} = 0$]. Thereby, the obtained values of $C_{d,LH}$ are in the range of the discharge coefficients C_d used for different greenhouse types without nets (Table 6). The discharge

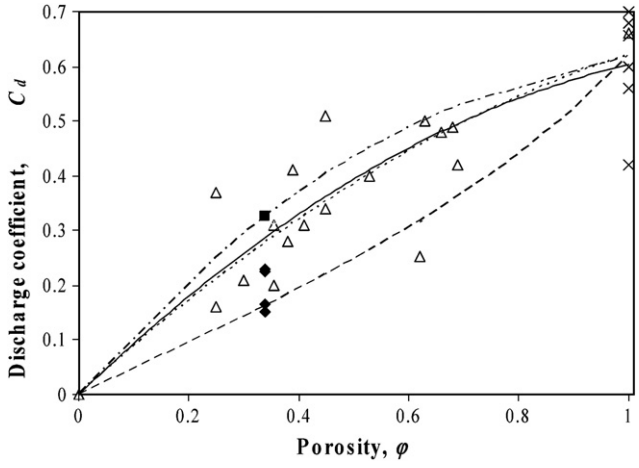

Fig. 7 – Discharge coefficients C_d *versus* insect-proof screen porosity φ. Values for the four tests in the Almería greenhouse (◆); values of screened openings measured by different authors presented in Table 7 (△); values of unscreened greenhouse used by different authors presented in Table 6 (×); value of C_d for the Almería greenhouse for $Re = 25$ (■); regression line fitted to all experimental data $C_d = -0.367\varphi^2 + 0.971\varphi$ with coefficient of determination $R^2 = 0.67$ (- - -); line calculated by Bailey *et al.* (2003) using Eqs. (14)–(16), and $F_\varphi = [18/Re + 0.75/\log(Re + 1.25) + 0.055\log(Re)]\,[(1 - \varphi^2)/\varphi^2]$ for $Re = 50$ (–·–), $Re = 25$ (- - -) and $Re = 5$ (– –), being $Re = Re_p d/K_p^{1/2}$ the Reynolds number based on the wire diameter of the net *d*.

coefficients due to the presence of screens in the greenhouse $C_{d,\varphi} = 0.156–0.245$ were calculated from the mean air velocity measured throughout the openings and the values of permeability $K_p = 2.37 \times 10^{-9}\ m^2$ and the inertial factor $Y = 0.243$ calculated using Eqs. (9) and (10) with values of a and b measured in the wind tunnel.

The mean total discharge coefficient $C_d = 0.194$ (Table 5) calculated for the Almería-type greenhouse with insect-proof screens (porosity $\varphi = 0.34$) from a wind-tunnel experiment using Eqs. (11)–(16) is similar to values obtained by several authors (Teitel *et al.*, 1999; Bailey *et al.*, 2003; Harmanto *et al.*, 2006) for nets with comparable porosities ($\varphi = 0.25–0.35$ in Table 7), as we can observe in Fig. 7. The values of C_d presented in Table 5 are also in good agreement with the total discharge coefficient calculated by Teitel *et al.* (2008) with $C_d = 0.253$ for a screened opening (porosity of 0.62). According to net properties, reductions in C_d seem proportional to the reduction of net porosity (Bailey *et al.*, 2003; Harmanto *et al.*, 2006) and the Reynolds number, as can be observed in Fig. 7. By a rough approximation, the reduction of greenhouse ventilation rate induced by the insect screens could be considered proportional to the reduction of airspeed measured at the side vent openings (Wang *et al.*, 1999). We can estimate the reduction of the wind-induced greenhouse ventilation rate from values of the discharge coefficient of the windows with and without the insect-proof screens (0.34 porosity) deduced from wind-tunnel measurements (Table 5). We can observe a reduction of the discharge coefficient ($C_d = 0.668$ without screens) of about 65% and 76% for measurements with strong ($C_d = 0.229$ for a wind speed $U_o = 7–9\ m\ s^{-1}$) and weak ($C_d = 0.159$ for a wind speed $U_o = 3–4\ m\ s^{-1}$) wind conditions, respectively.

3.4. *Estimation of the wind effect coefficient*

The dimensionless wind effect coefficient C_w expresses the translation of the wind field at reference level to the wind field near the opening (Kittas *et al.*, 1996). We have used Eqs. (1)–(3) to obtain C_w for the three ventilation models (M1, M2 and M3) derived from Bernoulli's equation (Boulard and Baille, 1995; Boulard *et al.*, 1997a; Kittas *et al.*, 1997). The mean C_w for the three ventilation models (Table 8) have been deduced from Eqs. (1)–(3) using the mean ventilation flows $\overline{G_M}(u*)$ (Table 4), calculated from Eq. (4) with scaled air velocity u^*, and the mean values of C_d obtained from wind-tunnel measurements (Table 5). The models that obtain a better fit to the experimental data are Model 1, considering the resulting pressure distribution as the sum of the pressure fields due to stack and wind effects, and the most simplified Model 3, with similar values of R^2 (Table 8). If the fluxes driven separately by the wind and stack effects are added together (Model 2), R^2 decreases by 1%. The mean values of the wind effect coefficient for model 1, $C_w = 0.049 \pm 0.016$ and model 2, $C_w = 0.022 \pm 0.017$, are much lower than values given in the literature for these models (Table 6). However, Pérez Parra *et al.* (2004) also obtained a small wind effect coefficient $C_w = 0.0017$ for a five-span Almería greenhouse with side and roof vent openings using Model 1 (Table 6).

The average value of C_w that we obtain with Model 3 is $C_w = 0.066 \pm 0.010$ (Table 8). This value is in good agreement

Table 8 – Values of the wind effect coefficients calculated for the four measurement series and the average value C_w corresponding to three models for calculating the mean ventilation volumetric flow rate in the greenhouse (mean ± standard deviation): C_w (M1) from Eq. (3), C_w (M2) from Eq. (4), C_w (M3) from Eq. (5)

Date	C_w (M1)	C_w (M2)	C_w (M3)	$E_V = C_d C_w^{0.5}$ (M3)	C_w' (M3)	C_{wSW} (M3)	C_{wSL} (M3)	C_{wRW} (M3)	C_{wRL} (M3)
Measurements with a Poniente wind from southwest									
04/02/2008	0.037	0.009	0.056	0.036	0.039	0.120	0.073	0.070	0.025
15/02/2008	0.034	0.005	0.076	0.046	0.036	0.125	0.054	0.116	0.099
Measurements with a Levante wind from northeast									
11/02/2008	0.054	0.030	0.059	0.056	0.013	0.033	0.079	0.072	0.025
13/02/2008	0.068	0.040	0.073	0.061	0.028	0.014	0.127	0.074	0.014
Mean	0.048 ± 0.016	0.021 ± 0.017	0.066 ± 0.010	0.050 ± 0.011	0.029 ± 0.012	0.073 ± 0.058	0.083 ± 0.031	0.083 ± 0.022	0.041 ± 0.039
R^2	0.984	0.975	0.985						

The overall wind and pressure drop related coefficient $E_V = C_d C_w^{0.5}$, the wind effect coefficient for the turbulence airflow C_w' have been calculated from Eq. (5). Wind effect coefficients for the windward side vent C_{wSW}, the leeward side vent C_{wSL}, the windward roof vent C_{wRW} and the leeward roof vent C_{wRL} have been calculated from Eq. (15).

Please cite this article in press as: Molina-Aiz, F.D. et al., A study of natural ventilation in an Almería-type greenhouse with insect screens by means of tri-sonic anemometry, Biosystems Engineering (2009), doi:10.1016/j.biosystemseng.2009.06.013

with $C_w = 0.071$ obtained by Kittas *et al.* (1996) and $C_w = 0.075$ by Teitel *et al.* (2008) for tunnel greenhouses with two continuous side openings. Overall, the value of the mean wind effect coefficient calculated in this work is in very good agreement with the one deduced from tracer gas measurements by Pérez Parra *et al.* (2004) for a similar Almería greenhouse with side and roof vent openings without insect-proof screens, $C_w = 0.074$. The wind effect model (Model 3) has the advantage of allowing the wind effect coefficients to be calculated individually for each vent opening.

The individual wind effect coefficients C_{wj} for each of the four vents j (Table 8) were based on the average scaled air velocity passing through them u_j^*, the discharge coefficients C_d of each one (Table 5) and the wind speed at reference height U_o (Table 1). We use the following equation:

$$C_{wj} = \left(\frac{\overline{u_j^*}}{C_d U_o}\right)^2 \quad (17)$$

For a *Poniente* wind, the ratio between the windward and leeward side vent coefficients $C_{wSW}/C_{wSL} = 1.99$ is similar to the value $C_{wSW}/C_{wSL} = 0.46/0.18$ found by Kamaruddin (1999), in a tunnel greenhouse with side and roof vents. Montero *et al.* (1997) also obtained great variability for values of the wind effect coefficient for roof vents open to the windward (0.32–0.48) and leeward sides (0.06–0.09) in a 1/3 scale model of a three-span greenhouse.

Model 3 supposes that the volumetric flow rate G is proportional to three parameters, as we can deduce from Eq. (3): the surface area of the vent openings S_V, the outside wind speed U_o and a coefficient of effectiveness of the openings $E_V = C_d C_w^{0.5}$. This coefficient $C_d C_w^{0.5}$ is frequently used in the literature to characterise the effect of wind on ventilation. For the Almería-type greenhouse we obtain here a mean value $C_d C_w^{0.5} = 0.050 \pm 0.011$, which is very similar to the value 0.052 obtained by Katsoulas *et al.* (2006) for a mono-span greenhouse with insect-proof screens of 50% porosity and the value calculated by Teitel *et al.* (2008) in a screened greenhouse. However, these values are lower than that found by Kittas *et al.* (2002) in a multispan greenhouse with insect-proof screens (0.6 porosity) on the roof vents. For the wind effect model (Model 3) they deduced an effectiveness coefficient for the window of $E_V = 0.136$, with a wind effect coefficient of $C_w = 0.169$ and a discharge coefficient of $C_d = 0.330$.

Fatnassi *et al.* (2002) indicated that the ratio between the ventilation rates for a greenhouse with and without screens could be considered proportional to the ratio between the discharge coefficients of their vents. The value for the above ratio calculated by Kittas *et al.* (2008) was 0.67, whereas they observed a ratio of 0.24 of the normalised air velocity measured near the vents. We have deduced the wind and pressure drop related coefficient for the greenhouse without nets, assuming that there is no screen on the openings ($C_d = C_{d,LH} = 0.668$) and using the mean wind effect coefficient $C_w = 0.067$ (Table 8) as proposed Teitel *et al.* (2008), obtaining a value of $E_V(C_{d,LH}) = C_{d,LH} C_w^{0.5} = 0.173$. This value is in good agreement with the values reported in the bibliography ranging from 0.07 to 0.27 for different greenhouse types equipped with non-screened side and roof openings (Table 6) and with the value $C_d C_w^{0.5} = 0.181$ deduced by Teitel *et al.* (2008) following the same procedure. Therefore, use of the anti-aphid insect screen in the

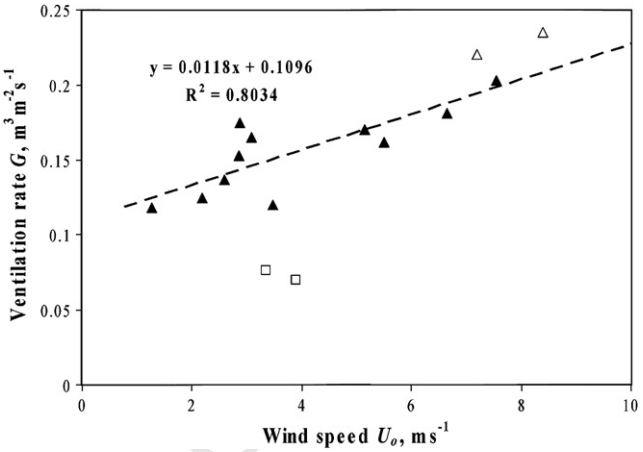

Fig. 8 – Ventilation rate per unit of vent opening area in Almería greenhouses with side vent openings and vents roof with insect-proof screen, calculated from tri-sonic anemometer measurements for Poniente (□) and Levante (△) winds, and without screen deduced by Pérez Parra *et al.* (2004) with tracer gas measurements (▲).

openings can cause approximately a 71% reduction of C_d and consequently of the wind-related coefficient $C_d C_w^{0.5}$. Katsoulas *et al.* (2006) reported a 33% reduction in the calculated wind-related coefficients, $C_d C_w^{0.5}$ being equal to 0.078 for the greenhouse without screen in the openings. For an Almería-type greenhouse, Pérez Parra *et al.* (2004) also observed that the increased resistance to airflow caused by an insect exclusion screen with a porosity of 0.39 fitted in the roof vents reduced ventilation by 37%. The ventilation rates per unit of vent opening area calculated in this work by sonic anemometry for a *Poniente* wind are approximately 50% of the value deduced by Pérez Parra *et al.* (2004) with tracer gas measurements for an Almería greenhouse without screens (Fig. 8).

The results obtained show that the wind effect coefficient of the Almería-type greenhouse (Table 8) is lower than those obtained in previous works on different greenhouse types (Table 6). These low C_w values could be partly attributed to the presence of mature plants (leaf area index of 1.6 $m^2\ m^{-2}$) that create a barrier between the two greenhouse side vents; and accordingly, significantly reduce the greenhouse ventilation rate (Katsoulas *et al.*, 2006). Boulard *et al.* (1997a) concluded that the presence of a crop decreased the value of $E_V = C_d C_w^{0.5}$ by as much as 28%. The low C_w values are also influenced by the proximity of obstacles to the greenhouses (an advertising sign close to the northeast side vent opening), as the pressure field of the airflow around it may be affected by adjacent buildings reducing the air velocity near vent openings (ASHRAE, 1993).

The wind effect model (Model 3) also allows us to calculate the wind effect coefficients for the turbulence airflow C_w', which describes the fluctuating characteristics of wind pressure (Boulard *et al.*, 1996). The values of C_w' (Table 8) have been deduced for the wind effect model (M3) from Eq. (3) using the turbulent ventilation flows G' (Table 4) calculated from Eq. (4) with direct measurement of air turbulence velocity u' at the vent openings. The measured turbulent wind effect coefficients C_w' are quite steady, with values of around half the mean wind effect coefficients C_w (Table 8), which indicates

Please cite this article in press as: Molina-Aiz, F.D. et al., A study of natural ventilation in an Almería-type greenhouse with insect screens by means of tri-sonic anemometry, Biosystems Engineering (2009), doi:10.1016/j.biosystemseng.2009.06.013

strong turbulence at the greenhouse openings. Boulard *et al.* (1998) observed absolute values of the same order of magnitude for the turbulent and mean coefficients.

4. Conclusions

Volumetric flow rate measurements performed in an Almería-type greenhouse are presented and analysed with reference to the combination of the two major physical driving forces of ventilation, the wind and buoyancy effects. The three models used give a good fit to the four experimental data, but considering the resulting airflow as the sum of the air fluxes due to buoyancy and wind effects (Model 2) we can improve the degree to which the mass conservation in the greenhouse is satisfied compared to the values calculated scaling the air velocity only with the wind speed (Model 3). The wind coefficient of the greenhouse has been calculated from the ventilation airflow by measuring air velocity through the openings with a tri-sonic anemometer. The results obtained with Model 3 $C_w = 0.066 \pm 0.010$ show that the wind effect coefficient of the greenhouse is lower than those obtained by previous works on different greenhouse types. This may be due to two important characteristics of the Almería-type greenhouse analysed in this work which make natural ventilation difficult: the presence of mature tomato plants inside the greenhouse and an obstacle close to one of the side vent openings, which affected the air movement through it.

Discharge coefficients due to the presence of insect-proof screens $C_{d,\varphi} = 0.156$–0.245 in the greenhouse were calculated from wind-tunnel measurements. The mean value of the discharge coefficient of the openings ($C_d = 0.193$) calculated for the Almería-type greenhouse with an insect-proof screen in the openings is similar to values obtained by several authors for windows with nets of comparable porosity. We have estimated that use of the anti-aphid insect screen in the openings can cause approximately a 71% reduction in the value of the wind-related coefficient $C_d C_w^{0.5}$ and therefore, in order to obtain the same ventilation flow as without screen, the vent opening area should be increased.

In the particular case of a five-span Almería-type greenhouse equipped with two continuous roof vents at the gutters and two side vent openings, a wind blowing perpendicular to the greenhouse ridge produces an inflow at the side vent opening free of obstacles and an outflow at the roof vents. At the side opening influenced by the proximity of an obstacle (an advertising sign close to the northeast side vent opening), the airflow depends on the wind direction (*Levante* or *Poniente*). When the side opening close to the sign is on the windward side of the greenhouse (for a *Levante* wind), air exits through the half of the window next to the obstacle, whereas in the other half of this side opening the air enters the greenhouse. However, when the side opening close to the obstacle is on the leeward side of the greenhouse, for a *Poniente* wind, air enters through the lower part of the opening and exits through the upper part.

The airflow patterns measured for *Poniente* wind are qualitatively in good agreement with the airflow patterns simulated with CFD and measured with an omnidirectional anemometer (Molina-Aiz *et al.*, 2004b) inside the same greenhouse with two side openings and with only one roof vent in the central ridge, and without the publicity sign close to the northeast side opening. Direct estimation of air velocity at the vent openings by means of tri-directional sonic anemometry measurements provided a spatial description of mean air velocities and turbulent flows. Turbulence intensity has a local maximum in the northeast side vent opening where the outflow interacts with inflow due to the nearby sign.

5. Uncited references

Tanny et al., 2008; Teitel, 2007.

Acknowledgements

The authors wish to express their gratitude to the Spanish Ministerio de Educación y Ciencia for partially financing the present work by means of the research grants AGL2006-09068/AGR and BIA2006-12323.

Appendix A. Air velocities scaled only with wind speed

As a first approximation, we have calculated an air velocity in the opening scaled taking only wind effect into account $\ddot{u}_j(t)$, multiplying measured values of air velocity $u_j(t)$ on the minute t at each point j in the greenhouse openings by the ratio between the average wind speed $\overline{U_o}$ for the overall test period (several hours) and the instantaneous values $U_o(t)$ (average for each minute t):

$$\ddot{u}_j(t) = u_j(t)\frac{\overline{U_o}}{U_o(t)} \tag{18}$$

The use of Eq. (18) is based on the assumption that the contribution of stack effect is negligible and that the variations of the air velocity through the greenhouse openings are directly proportional to the outside wind speed variations (Model 3).

Appendix B. Air velocities scaled with wind speed and temperature differences

During the experiment there were variations not only in wind speed (as the first approximation in Appendix A supposes), but also in the buoyancy effect. To take into account the effect of the evolution of the inside–outside temperature difference throughout the experiment on the air velocity at the greenhouse openings, we have used the volumetric flow rate G calculated with the second ventilation model (considering that the resulting flux is the sum of two independent fluxes) as scaling parameter. For this second approach, we have calculated a scaled air velocity in the opening $u_j^*(t)$ taking buoyancy and wind effects into account, multiplying measured values of air velocity $u_j(t)$ by the ratio between the volumetric flow rate calculated with Eq. (2) using average values of the outside temperature, the outside–inside temperature gradient and the wind speed $(\overline{T_o}, \overline{\Delta T_{io}}, \overline{U_o})$ for the overall test period (several hours) and using the instantaneous values $[T_o(t), \Delta T_{io}(t), U_o(t)]$ (average for each minute t), respectively:

Please cite this article in press as: Molina-Aiz, F.D. et al., A study of natural ventilation in an Almería-type greenhouse with insect screens by means of tri-sonic anemometry, Biosystems Engineering (2009), doi:10.1016/j.biosystemseng.2009.06.013

$$\text{style}u_j^*(t) = u_j(t)\frac{\overline{G}}{G(t)}\frac{= u_j(t)C_d\dfrac{S_{VR}S_{VS}}{\sqrt{S_{VR}^2+S_{VS}^2}}\sqrt{2g\dfrac{\overline{\Delta T_{io}}}{\overline{T_o}}h_{SR}}+\dfrac{S_{VR}+S_{VS}}{2}C_d\sqrt{\overline{C_w}}\,\overline{U_o}}{C_d\dfrac{S_{VR}S_{VS}}{\sqrt{S_{VR}^2+S_{VS}^2}}\sqrt{2g\dfrac{\Delta T_{io}(t)}{T_o(t)}h_{SR}}+\dfrac{S_{VR}+S_{VS}}{2}C_d\sqrt{C_w}U_o(t)} = \frac{A\sqrt{B\dfrac{\overline{\Delta T_{io}}}{\overline{T_o}}}+C\overline{U_o}}{A\sqrt{B\dfrac{\Delta T_{io}(t)}{T_o(t)}}+CU_o(t)} \quad (19)$$

From the equality presented in Eq. (19) we can deduce the values of parameters A, B and C for the four tests:

$$A = C_d\frac{S_{VR}S_{VS}}{\sqrt{S_{VR}^2+S_{VS}^2}} \quad (20)$$

$$B = 2gh_{SR} \quad (21)$$

$$C = \frac{S_{VR}+S_{VS}}{2}C_d\sqrt{C_w} \quad (22)$$

We have used these equations in an iterative process obtaining the values of the parameter A, B and C (Table 4) to calculate the wind effect coefficient C_w from air velocities u^* scaled with the ventilation flux.

REFERENCES

Abreu P E; Boulard T; Mermier M; Meneses J F (2006). Parameter estimation and selection of a greenhouse natural ventilation model and its use on an energy balance model to estimate the greenhouse air temperature. Acta Horticulturae, **691**, 611–618.

Arbel A; Shklyar A; Barak M (2000). Buoyancy-driven ventilation in a greenhouse cooled by a fogging system. Acta Horticulturae, **534**, 327–334.

ASHRAE (1993). Airflow around buildings. In, **Vol 14**, pp. 14.1–14.3. American Society of Heating, Refrigerating, and Air-Conditioning Engineers, Atlanta, USA.

Bailey B J; Montero J I; Pérez-Parra J; Robertson A P; Baeza E; Kamaruddin R (2003). Airflow resistance of greenhouse ventilators with and without insect screens. Biosystems Engineering, **86**(2), 217–229. doi:10.1016/S1537-5110(03)00115-6.

Baptista F J; Bailey B J; Randall J M; Meneses J F (1999). Greenhouse ventilation rate: theory and measurement with tracer gas techniques. Journal of Agricultural Engineering Research, **72**, 363–374. doi:10.1006/jaer.1998.0381.

Bartzanas T; Boulard T; Kittas C (2002). Numerical simulation of the airflow and temperature distribution in a tunnel greenhouse equipped with insect-proof screen in the openings. Computer and Electronic in Agriculture, **34**, 207–221.

Bartzanas T; Boulard T; Kittas C (2004). Effect of vent arrangement on windward ventilation of a tunnel greenhouse. Biosystems Engineering, **88**(4), 479–490. doi:10.1016/j.biosystemseng.2003.10.006.

Baetke F; Werner H; Wengle H (1990). Numerical simulation of turbulent flow over surface-mounted obstacles with sharp edges and corners. Journal of Wind Engineering and Industrial Aerodynamics, **35**(1–3), 129–147.

Bhattacharyya S; Maiti D K (2004). Shear flow past a square cylinder near a wall. International Journal of Engineering Science, **42**, 2119–2134. doi:10.1016/j.ijengsci.2004.04.007.

Bot G P A (1983). Greenhouse climate: from physical processes to a dynamic model. Ph.D. thesis, Agricultural University of Wageningen, The Netherlands.

Boulard T; Baille A (1995). Modelling of air exchange rate in a greenhouse equipped with continuous roof vents. Journal of Agricultural Engineering Reserch, **61**(1), 37–48.

Boulard T; Draoui B (1995). Natural ventilation of a greenhouse with continuous roof vents: measurements and data analysis. Journal of Agricultural Engineering Research, **61**(1), 27–36.

Boulard T; Meneses J F; Mermier M; Papadakis G (1996). The mechanisms involved in the natural ventilation of greenhouses. Agricultural and Forest Meteorology, **79**, 61–77.

Boulard T; Feuilloley P; Kittas C (1997a). Natural ventilation performance of six greenhouse and tunnel types. Journal of Agricultural Engineering Research, **67**(4), 249–266.

Boulard T; Kittas C; Papadakis G; Mermier M (1998). Pressure field and airflow at the opening of a naturally ventilated greenhouse. Journal of Agricultural Engineering Research, **71**(1), 93–102.

Boulard T; Papadakis G; Kittas C; Mermier M (1997b). Air flow and associated sensible heat exchanges in a naturally ventilated greenhouse. Agricultural and Forest Meteorology, **88**(1–4), 111–119.

Boulard T; Wang S; Haxaire R (2000). Mean and turbulent air flows and microclimatic patterns in an empty greenhouse tunnel. Agricultural and Forest Meteorology, **100**(2–3), 169–181.

Bournet P E; Ould Khaoua S A; Boulard T; Migeon C; Chassériaux G (2007). Effect of roof and side opening combinations on the ventilation of a greenhouse using computer simulation. Transactions of the ASABE, **50**(1), 201–212.

Bruce J M (1978). Natural convection through openings and its applications to cattle building ventilation. Journal of Agricultural Engineering Research, **23**(2), 151–167.

Demrati H; Boulard T; Bekkaoui A; Bouirden L (2001). Natural ventilation and microclimatic performance of a large-scale banana greenhouse. Journal of Agricultural Engineering Research, **80**(3), 261–271.

Dierickx W (1998). Flow reduction of synthetic screens obtained with both a water and airflow apparatus. Journal of Agricultural Engineering Research, **71**(1), 67–73.

Fatnassi H; Boulard T; Lagier J (2004). Simple indirect estimation of ventilation and crop transpiration rates in a greenhouse. Biosystems Engineering, **88**(4), 467–478. doi:10.1016/j.biosystemseng.2004.05.003.

Fatnassi H; Boulard T; Bouirden L (2003). Simulation of climatic conditions in full-scale greenhouse fitted with insect-proof screens. Agricultural and Forest Meteorology, **118**(1–2), 97–111. doi:10.1016/S0168-1923(03)00071-6.

Fatnassi H; Boulard T; Demrati H; Bouirden L; Sappe G (2002). Ventilation performance of a large Canarian-type greenhouse equipped with insect-proof nets. Biosystems Engineering, **82**(1), 97–105. doi:10.1006/bioe.2001.0056.

Fatnassi H; Boulard T; Poncet C; Chave M (2006). Optimisation of greenhouse insect screening with computational fluid dynamics. Biosystems Engineering, **93**(3), 301–312. doi:10.1016/j.biosystemseng.2005.11.014.

Fernandez J E; Bailey B J (1992). Measurement and prediction of greenhouse ventilation rates. Agricultural and Forest Meteorology, **58**(3–4), 229–245.

Forchheimer P (1901). Wasserbewegung durch Boden. [Water-movement from ground]. Zeitschrift des Vereines Deutscher Ingenieure, **45**, 1782–1788.

Fitzgerald S D; Woods A W (2007). On the transition from displacement to mixing ventilation with a localized heat source.

Please cite this article in press as: Molina-Aiz, F.D. et al., A study of natural ventilation in an Almería-type greenhouse with insect screens by means of tri-sonic anemometry, Biosystems Engineering (2009), doi:10.1016/j.biosystemseng.2009.06.013

Building and Environment, **42**(6), 2210–2217. doi:10.1016/j.buildenv.2006.09.012.

Harmanto; **Tantau H J; Salokhe V M** (2006). Microclimate and air exchange rates in greenhouses covered with different nets in the humid tropics. Biosystems Engineering, **94**(2), 239–253. doi:10.1016/j.biosystemseng.2006.02.016.

Haslavsky V; Tanny J; Teitel M (2006). Interaction between the mixing and displacement modes in a naturally ventilated enclosure. Building and Environment, **41**(12), 1755–1761. doi:10.1016/j.buildenv.2005.07.013.

Jiménez-Hornero F J; Gutiérrez de Ravé E; Hidalgo R; Giráldez J V (2005). Numerical study of the natural airflow in greenhouses using a two-dimensional lattice model. Biosystems Engineering, **91**(2), 219–228. doi:10.1016/j.biosystemseng.2005.03.003.

Kamaruddin R (1999). A naturally ventilated crop protection structure for tropical conditions. Ph.D. thesis, University of Cranfield, Cranfield, United Kingdom.

Katsoulas N; Bartzanas T; Boulard T; Mermier M; Kittas C (2006). Effect of vent openings and insect screens on greenhouse ventilation. Biosystems Engineering, **93**(4), 427–436. doi:10.1016/j.biosystemseng.2005.01.001.

Katsoulas N; Baille A; Kittas C (2007). Leaf boundary layer conductance in ventilated greenhouses: an experimental approach. Agricultural and Forest Meteorology, **144**(3–4), 180–192. doi:10.1016/j.agrformet.2007.03.003.

Kittas C; Katsoulas N; Bartzanas T; Boulard T; Mermier M (2006). Effect of vent opening and insect screens on greenhouse microclimate distribution. Acta Horticulturae, **719**, 615–622.

Kittas C; Boulard T; Bartzanas T; Katsoulas N; Mermier M (2002). Influence of an insect screen on greenhouse ventilation. Transactions of the ASAE, **45**(4), 1083–1090.

Kittas C; Boulard T; Mermier M; Papadakis G (1996). Wind induced air exchange rates in a greenhouse tunnel with continuous side openings. Journal of Agricultural Engineering Research, **65**(1), 37–49.

Kittas C; Boulard T; Papadakis G (1997). Natural ventilation of a greenhouse with ridge and side openings: sensitivity to temperature and wind effects. Transactions of the ASAE, **40**(2), 415–425.

Kittas C; Draoui B; Boulard T (1995). Quantification du taux d'aération d'une serre á ouvrant continu en toiture. Agricultural and Forest Meteorology, **77**(1–2), 95–111.

Kittas C; Katsoulas N; Bartzanas T; Mermier M; Boulard T (2008). The impact of insect screens and ventilation openings on the greenhouse microclimate. Transactions of the ASABE, **51**(6), 2151–2165.

Kosmos S R; Riskowski G L; Christianson L L (1993). Force and static pressure resulting from airflow through screens. Transactions of the ASAE, **36**(5), 1467–1472.

Kuciauskas A P; Brody L R; Hadjimichael M; Bankert R L; Tag P M; Peak J E (1998). A fuzzy expert system to assist in the prediction of hazardous wind conditions within the Mediterranean basin. Meteorological Applications, **5**(4), 307–320. doi:10.1017/S1350482798001005.

Miguel A F; Van de Braak N J; Bot G P A (1997). Analysis of the airflow characteristics of greenhouse screening materials. Journal of Agricultural Engineering Research, **67**(2), 105–112.

Molina-Aiz F D; Valera D L; Álvarez A J (2004a). Using computational fluid dynamics tool to model the internal climate of an Almería-type greenhouse. Acta Horticulturae, **654**, 271–278.

Molina-Aiz F D; Valera D L; Álvarez A J (2004b). Measurement and simulation of climate inside Almería-type greenhouses using computational fluid dynamics. Agricultural and Forest Meteorology, **125**, 33–51. doi:10.1016/j.agrformet.2004.03.009.

Molina-Aiz F D; Valera D L; Álvarez A J; Madueño A (2006). A wind tunnel study of airflow through horticultural crops: determination of the drag coefficient. Biosystems Engineering, **93**(4), 447–457. doi:10.1016/j.biosystemseng.2006.01.016.

Molina-Aiz F D; Valera D L; Lopez A; Álvarez A J (2009). Estudio de la ventilación natural en un invernadero tipo Almería mediante anemometría sónica triaxial. (A study of natural ventilation in an Almería-type greenhouse with tri-sonic anemometry). In: Actas del V Congreso Nacional y II Congreso Ibérico AGROINGENIERÍA 2009, Paper: congr-2009-69, 12 pp, Lugo, Spain.

Molina-Aiz F D; Valera D L; Gil J A; Peña A A (2005). Optimization of Almeria-type greenhouse ventilation performance with computational fluid dynamics. Acta Horticulturae, **691**, 433–440.

Montero J I; Muñoz P; Anton A (1997). Discharge coefficients of greenhouse windows with insect-proof screens. Acta Horticulturae, **443**, 71–77.

Muñoz P; Montero J I; Antón A; Giuffrida F (1999). Effect of insect-proof screens and roof openings on greenhouse ventilation. Journal of Agricultural Engineering Research, **73**, 171–178. doi:10.1006/jaer.1998.0404.

Nield D A; Bejan A (1999). Convection in Porous Media. Springer, New Cork, USA.

Papadakis G; Mermier M; Meneses J F; Boulard T (1996). Measurement and analysis of air exchange rates in a greenhouse with continuous roof and side openings. Journal of Agricultural Engineering Research, **63**(3), 219–228.

Pérez Parra J; Baeza E; Montero J I; Bailey B J (2004). Natural ventilation of parral greenhouses. Biosystems Engineering, **87**(3), 89–100. doi:10.1016/j.biosystemseng.2003.12.004.

Sase S; Christianson L L (1990). Screening greenhouses – some engineering considerations. In Proceeding of the 1990 Northeast Agricultural/Biological Engineering Conference. ASAE, Pennsylvania, USA. Paper No. NABEC: 90-201.

Sase S; Reiss E; Both A J; Roberts W J (2002). A natural ventilation model for open-roof greenhouses. In ASAE International Meeting/CIGR XVth World Congress. ASAE, Chicago, USA. Paper No.: 024010.

Sbita L; Boulard T; Mermier M (1996). Natural ventilation performance of a greenhouse tunnel in south Tunisia. In: Cultures protégées dans la région méditerranéenne: Actes du Colloque d'Agadir. Cahiers Options Méditerranéens, Vol. 31, pp 109–118, Agadir, Morocco.

Simiu E; Scanlan R H (1996). Wind Effects on Structures: Fundamentals and Applications to Design. John Wiley & Sons, New York, USA. 704 pp.

Soni P; Salokhe V M; Tantau H J (2005). Effect of screen mesh size on vertical temperature distribution in naturally ventilated tropical greenhouses. Biosystems Engineering, **92**(4), 469–482. doi:10.1016/j.biosystemseng.2005.08.005.

Tanny J; Cohen S; Teitel M (2003). Screenhouse microclimate and ventilation: an experimental study. Biosystems Engineering, **84**(3), 331–341. doi:10.1016/S1537-5110(02)00288-X.

Tanny J; Haijun L; Cohen S (2006). Airflow characteristics, energy balance and eddy covariance measurements in a banana screenhouse. Agricultural and Forest Meteorology, **139**(1–2), 105–118. doi:10.1016/j.agrformet.2006.06.004.

Tanny J; Haslavsky V; Teitel M (2008). Airflow and heat flux through the vertical opening of buoyancy-induced naturally ventilated enclosures. Energy and Buildings, **40**(4), 637–646. doi:10.1016/j.enbuild.2007.04.020.

Teitel M (2001). The effect of insect-proof screens in roof openings on greenhouse microclimate. Agricultural and Forest Meteorology, **110**(1), 13–25.

Teitel M (2007). The effect of screened openings on greenhouse microclimate. Agricultural and Forest Meteorology, **143**(3–4), 159–175. doi:10.1016/j.agrformet.2007.01.005. Q6

Teitel M; Barak M; Berlinger M J; Lebiush-Mordechai S (1999). Insect-proof screens in greenhouses: their effect on roof ventilation and insect penetration. Acta Horticulturae, **507**, 25–34.

Please cite this article in press as: Molina-Aiz, F.D. et al., A study of natural ventilation in an Almería-type greenhouse with insect screens by means of tri-sonic anemometry, Biosystems Engineering (2009), doi:10.1016/j.biosystemseng.2009.06.013

Teitel M; Liran O; Tanny J; Barak M (2008). Wind driven ventilation of a mono-span greenhouse with a rose crop and continuous screened side vents and its effect on flow patterns and microclimate. Biosystems Engineering, **101**(1), 111–122. doi:10.1016/j.biosystemseng.2008.05.012.

Teitel M; Shklyar A (1998). Pressure drop across insect-proof screens. Transactions of the ASAE, **41**(6), 1829–1834.

Teitel T; Tanny J; Ben-Yakir D; Barak M (2005). Airflow patterns through roof openings of a naturally ventilated greenhouse and their effect on insect penetration. Biosystems Engineering, **92**(3), 341–353. doi:10.1016/j.biosystemseng.2005.07.013.

Valera D L; Álvarez A J; Molina-Aiz F D (2006). Aerodynamic analysis of several insect-proof screens used in greenhouses. Spanish Journal of Agricultural Research, **4**(4), 273–279.

Wang S; Boulard T (2000). Predicting the microclimate in a naturally ventilated plastic house in a Mediterranean climate. Journal of Agricultural Engineering Research, **75**(1), 27–38. doi:10.1006/jaer.1999.0482.

Wang S; Deltour J (1997). Natural ventilation induced airflow patters measured by an ultrasonic anemometer in Venlo-type greenhouse openings. Agricultural Engineering Journal, **6**, 185–196.

Wang S; Deltour J (1999). Lee-side ventilation-induced air movement in a large-scale multi-span greenhouse. Journal of Agricultural Engineering Research, **74**, 103–110. doi:10.1006/jaer.1999.0441.

Zhang J S; Janni K A; Jacobson L D (1989). Modeling natural ventilation induced by combined thermal buoyancy and wind. Transactions of the ASAE, **32**(6), 2165–2174.

Please cite this article in press as: Molina-Aiz, F.D. et al., A study of natural ventilation in an Almería-type greenhouse with insect screens by means of tri-sonic anemometry, Biosystems Engineering (2009), doi:10.1016/j.biosystemseng.2009.06.013